

TS
414

EFFECT OF TOOL LENGTH ON PLAIN TURNING PERFORMANCE

NORFAIZAH BIN IBRAHIM

Hak Milik MARA

UNIVERSITI TEKNOLOGI MALAYSIA

UNIVERSITI TEKNOLOGI MALAYSIA

DECLARATION OF THESIS / ~~UNDERGRADUATE PROJECT PAPER~~ AND COPYRIGHT

Author's full name : NORFAIZEM BIN IBRAHIM
 Date of birth : 14TH MARCH 1978
 Title : EFFECT OF TOOL LENGTH ON PLAIN TURNING
 PERFORMANCE
 Academic Session : 2009 / 2010

I declare that this thesis is classified as :

CONFIDENTIAL

(Contains confidential information under the Official Secret Act 1972)*

RESTRICTED

(Contains restricted information as specified by the organization where research was done)*

OPEN ACCESS

I agree that my thesis to be published as online open access (full text)

I acknowledged that Universiti Teknologi Malaysia reserves the right as follows:

- 1 The thesis is the property of Universiti Teknologi Malaysia.
- 2 The Library of Universiti Teknologi Malaysia has the right to make copies for the purpose of research only.
- 3 The Library has the right to make copies of the thesis for academic exchange.



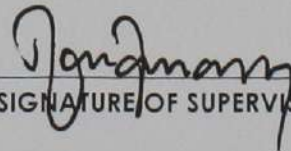
SIGNATURE

780314-02-6079

(NEW IC NO. /PASSPORT NO.)

Date : 10TH MAY 2010

Certified by :



SIGNATURE OF SUPERVISOR

PROF. DR. NOORDIN MOHD YUSOF

NAME OF SUPERVISOR

Date : 10TH MAY 2010**NOTES :**

If the thesis is CONFIDENTIAL or RESTRICTED, please attach with the letter from the organization with period and reasons for confidentiality or restriction.

**School of Graduate Studies
Universiti Teknologi Malaysia**

VALIDATION OF E-THESIS PREPARATION

Title of the thesis : EFFECT OF TOOL LENGTH ON PLAIN TURNING PERFORMANCE

Degree : MASTER OF ENGINEERING (MECHANICAL - ADVANCED
MANUFACTURING TECHNOLOGY)

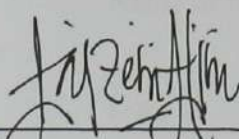
Faculty : MECHANICAL ENGINEERING

Year : 2009 / 2010

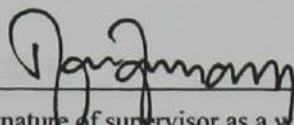
I NORFAIZEM BIN IBRAHIM (780314-02-6079)

(CAPITAL LETTER)

declare and verify that the copy of e-thesis submitted is in accordance to the Electronic Thesis and
Dissertation's Manual, School of Graduate Studies, UTM



(Signature of the student)



(Signature of supervisor as a witness)

Permanent address:

Kolej Kemahiran Tinggi MARA

Genting, 11000 Balik Pulau,

Pulau Pinang.

Name of Supervisor:

PROF. DR. NOORDIN MOHD YUSOF

Faculty:

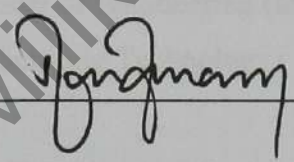
MECHANICAL ENGINEERING

Note: This form must be submitted to SPS together with the CD.

DECLARATION OF SUPERVISOR

DECLARATION OF SUPERVISOR

"I hereby, declare that I have read this thesis and in my opinion this thesis is sufficient in terms of scope and quality for the award of degree of Master of Engineering (Mechanical – Advanced Manufacturing Technology)"

Signature : 
Name of Supervisor : PROF. DR. NOORDIN MOHD YUSOF
Date : 10TH MAY 2010

Hak Milik MARA

Faculty of Mechanical Engineering
Universiti Teknologi MARA

MAY 2010

EFFECT OF TOOL LENGTH ON PLAIN TURNING PERFORMANCE

NORFAIZEM BIN IBRAHIM

A project report submitted in partial fulfillment of the requirements for
the award of the degree of Master of Engineering (Mechanical -
Advanced Manufacturing Technology)

Faculty of Mechanical Engineering
Universiti Teknologi Malaysia

MAY 2010

I declare that this thesis entitled "*Effect of Tool Length on Plain Turning Performance*" is the result of my own research except as cited in the references. The thesis has not been accepted for any degree and is not concurrently submitted in candidature of any other degree.

Signature : 

Name : NORFAIZEM BIN IBRAHIM

Date : 10TH MAY 2010

ACKNOWLEDGEMENTS

In the name of Allah, the most Gracious and most Compassionate

I thank Allah for the blessings and giving me strength to complete this paper. I am indebted to all who helped directly or indirectly to complete this paper.

Thanks are due to my wife, Anisah, and my daughter, Tingi MARA, for their love and support during the period of this research work.

To my beloved wife and daughter

To my beloved parents who taught me life by doing

Hak Milk MARA

ACKNOWLEDGEMENTS

In the name of Allah, the most Gracious and most Compassionate

I would like to thank Allah Almighty for the blessings and giving me strength to complete this thesis. I am indebted to all who helped directly or indirectly to complete this project report.

Thanks are due to Majlis Amanah Rakyat and Kolej Kemahiran Tinggi MARA Balik Pulau for the financial and facilities support during the period of this research work.

I would like to thank Prof. Dr. Noordin Mohd Yusof (supervisor) and others lecturers in this programme for their valuable experiences, comments, suggestions, guidance and advice throughout the project. There are no doubts that their valuable comments and suggestions have influenced and enhanced this project report.

A special thanks are due to many other individuals and organizations that have been involved with this project in one form or another.

Last but certainly not least, very special thanks are due to my family and friends who supported me from start to finish with their love, support and encouragement are greatly appreciated.

ABSTRACT

The purpose of this research paper is to find a correlation between surface roughness and cutting conditions (cutting speed, feed rate, depth of cut, and tool overhang) especially tool overhang as the output response variable in turning Aluminum Alloy 6061 without using supported (tailstock) and in dry cutting (without coolant). The tool length variable is introduced because to investigate that the vibration generated by varying the tool length could affect the resulting surface finish. Dry cutting (without using cutting fluid) are conducted to stimulate a good turning, provide a clean environment to obtain undisturbed clear cutting vibration, which result in more accurate and clear correlation between cutting condition and surface roughness. Examine the relationship that exists between the length, at a specific diameter, and surface roughness of bar stock in unsupported turning operations in an attempt to reduce setup waste in turning operations. The concept of Design of Experiments (DOE) was used for necessary experimentation. The experimental results were analyzed statistically to study the influence of process parameters on surface roughness. Response surface methodology (RSM) was used for modeling and analysis in applications where a response of interest is influenced by several variables and the objective is to optimize this response under the range of cutting condition been set. The analysis of variance revealed in this study is that feed rate, cutting speed and tool length have significance effects on the surface roughness and the best surface roughness condition is achieved at a low feed rate 0.07 mm/rev, high cutting speed 280 m/min and short tool length 22 mm. The results also show that the feed rate has big effect on surface roughness followed by tool overhang and cutting speed. The depth of cut has not a significant effect on surface roughness in this study.

ABSTRAK

Tujuan kertas kajian ini adalah untuk mencari satu hubungkait antara kekasaran permukaan dan parameter pemotongan (kederasan memotong, kadar suapan, kedalaman potongan, dan juntaian matalat) terutama pembolehkan juntaian matalat dalam melarik Aloi Aluminium 6061 tanpa menggunakan penyokong (stok belakang) dan tanpa bendalir penyejuk. Panjang alat pembolehkan diperkenalkan untuk menyiasat samada getaran yang terhasil daripada pelbagai kepanjangan matalat akan mempengaruhi kemas permukaan bahan. Pemotongan tanpa bendalir penyejuk dijalankan bagi merangsang pemotongan larik yang baik, menyediakan persekitaran potongan yang tidak terganggu oleh bendalir penyejuk dimana hubungkait antara parameter pemotongan dan kekasaran permukaan adalah lebih jelas dan tepat. Ujikaji dijalankan tanpa penyokong (stok belakang) bertujuan mengurangkan pembaziran ketika penyediaan proses pemotongan bahan. Konsep Rekabentuk Eksperimen (DOE) digunakan untuk keperluan eksperimen ini. Keputusan percubaan dianalisis secara statistik untuk mempelajari pengaruh parameter terhadap kekasaran permukaan. Respon Metodologi Permukaan (RSM) digunakan bagi memastikan parameter yang mempengaruhi permukaan kekasaran dan mencari optimum parameter keatas respond dalam julat keadaan pemotongan yang telah ditetapkan. Analisis varian mendedahkan dalam kajian ini kadar suapan, kederasan pemotongan dan juntaian matalat memberikan kesan signifikansi terhadap kekasaran permukaan dan keadaan permukaan berada pada tahap yang baik apabila kadar suapan berada pada keadaan paling rendah iaitu 0.07 mm/rev, kederasan pemotongan pada tahap tertinggi 280 m/min dan juntaian matalat paling pendek 22 mm. Keputusan ujikaji juga menunjukkan bahawa kadar suapan merupakan pemberi kesan yang besar terhadap kekasaran permukaan diikuti juntaian matalat dan kederasan pemotongan. Kedalaman pemotongan tidak memberi kesan terhadap kekasaran permukaan dalam ujikaji ini.

TABLE OF CONTENTS

CHAPTER	TITLE	PAGE
	DECLARATION	ii
	DEDICATION	iii
	ACKNOWLEDGEMENTS	iv
	ABSTRACT	v
	ABSTRAK	vi
	TABLE OF CONTENTS	vii
	LIST OF TABLES	x
	LIST OF FIGURES	xi
	LIST OF ABBREVIATIONS AND SYMBOLS	xiii
	LIST OF APPENDICES	xiv
1	INTRODUCTION	1
	1.1 Overview	1
	1.2 Background and Rationale	3
	1.2.1 Research Objective	4
	1.3 Research Problem	4
	1.3.1 Statement of Research Problem	4
	1.3.2 Research Questions	5
	1.4 Dependent and Independent Variable	5
	1.5 Scope of Study	6
2	LITERATURE REVIEW	7
	2.1 Introduction	7

CHAPTER	TITLE	PAGE
2.2	Single Point Machining	8
	2.2.1 Introduction	8
	2.2.2 Cutting Data	9
2.3	Aluminum Alloys	12
	2.3.1 Introduction	12
	2.3.2 Machining	13
	2.3.3 Anodizing	13
	2.3.4 Joining	14
2.4	Surface Roughness	17
	2.4.1 Arithmetical Mean Roughness (Ra)	17
	2.4.2 Maximum Peak (Ry)	18
	2.4.3 Ten-point Mean Roughness (Rz)	19
2.5	Process Design	21
	2.5.1 Introduction	21
	2.5.2 Guidelines for Designing Experiments	23
	2.5.3 Factorial Experiments	24
2.6	Process Optimization	29
	2.6.1 Introduction	29
	2.6.2 Response Surface Methods and Designs	30
	2.6.3 The Method of Steepest Ascent	31
	2.6.4 Analysis of a Second-Order	33
3	METHODOLOGY	34
3.1	Introduction	34
	3.1.1 CNC Turning - DMG CTX 310	35
	3.1.2 External Tool Holder - PDJNL2020-43	37
	3.1.3 Indexable Inserts For Turning	38
	3.1.4 Mitutoyo Surface Roughness Tester SJ-400	39
3.2	RSM Methodology	40
	3.2.1 Test for signify. of the regression model	41

CHAPTER	TITLE	PAGE
	3.2.2 Test for significance on individual model coefficients	42
	3.2.3 Lack-of-Fit	42
	3.2.3 R-Square	43
	3.3 Experimental Setup	43
4	RESULT AND DISCUSSION	50
	4.1 Strategy of Experiment	50
	4.2 Central Composite Design (CCD)	54
	4.3 Confirmation Test	64
	4.4 Discussion	65
	4.4.1 Interaction between Tool Overhang, D and Feed Rate, B	65
	4.4.2 Cutting Speed	66
	4.4.3 Depth of Cut	67
	4.5 Tool Wear	68
	4.5.1 Table of Tool Wear Data for Actual Experiment	69
	4.5.2 Discussion	73
	4.6 Chip Formation	75
	4.6.1 Table of Chip Form Data for Actual Experiment	77
	4.6.2 Discussion	79
5	CONCLUSION	81
	5.1 Why Tool Length is been Investigate?	81
	5.2 Recommendations	83
	REFERENCE	84
	Appendices A-C	87-97

LIST OF TABLE

TABLE NO.	TITLE	PAGE
2.3.4.1	6061 Temper Designations and Definitions	14
2.3.4.2	Average Coefficient of Thermal Expansion (68 ⁰ to 212 ⁰ F) = 13.2×10^{-6} (inch per inch per ⁰ F)	14
2.3.4.3	Alloy 6061 Capabilities and Mechanical Property Limits	15
2.4	Surface Finish Tolerance in Manufacturing	20
2.5.3	Signs for effects in the 2 ³ design	28
3.3.1	Test matrix	47
3.3.2	The level of independent variables for the procedures	48
3.3.3	The cutting conditions and the groups of experimental testing	49
4.1.1	Data for surface finish data by using Full Factorial	51
4.1.2	ANOVA table show significant curvature	52
4.2.1	Data for surface finish data by using RSM	55
4.2.2	The table show quadratic model is suggested.	56
4.2.3	ANOVA table for response surface quadratic model	57
4.2.4	ANOVA table for R-square	58
4.2.5	Numerical optimization table found 21 solutions	62
4.3	Confirmation table	64
4.5.1.1	Table of Tool Wear Data for Actual Experiment	69
4.5.1.2	Comparison of Tool Wear (Crater Wear on Rake Face)	74
4.6.1.1	Table of chip formation data for actual experiment	77
4.6.1.2	Comparison of Chip Formation	80
5.2	Future Unsupported Workpiece in Dry Cutting	83

LIST OF FIGURE

FIGURE NO.	TITLE	PAGE
1.1	Fishbone diagram with factors that influence on surface roughness	2
2.2.2	The main cutting data/tool elements for turning tool applications	12
2.3.4	Comparative Characteristics of Related Alloys/Tempers	16
2.4.1	Arithmetical Mean Roughness (Ra) graph	18
2.4.2	Maximum Peak (Ry) graph	18
2.4.3	Ten-point Mean Roughness (Rz) graph	19
2.5.1	General model of a process	21
2.5.3.1	The 2^3 factorial design	24
2.5.3.2	Geometric presentation of contracts corresponding to the main effects and interaction in the 2^3 design	27
2.6.3	First order response surface and path of steepest ascent	32
3.1.1.1	CNC Turning DMG CTX 310 Glidimiester	35
3.1.1.2	Technical Data for CNC Turning DMG CTX 310 Glidimiester	36
3.1.2	Tool Holders for Negative Insert	37
3.1.3	Indexable Inserts for Turning	38
3.1.4.1	Mitutoyo Surface Roughness Tester SJ-400	39
3.1.4.2	Surface Roughness compensation	40
3.3.1	Illustration of workpiece dimension	44
3.3.2	Experimental setup	45
3.3.3	Factorial 2^4 design for the surface finish experiment	46
4.1	Flow chart strategy of experiment	53

FIGURE NO.	TITLE	PAGE
4.2.1	Illustration of workpiece dimension	54
4.2.2	The normal probability plots of residuals for surface roughness	59
4.2.3	The plots of the residuals versus the predicted response for surface roughness	60
4.2.4	Ra contours in feed-tool length plane at cutting speed of 230 m/min and depth of cut 0.15 mm	61
4.2.5	3D surface model in feed-tool length plane at cutting speed of 230 m/min and depth of cut 0.15 mm	61
4.2.6	Desirability contours in feed-tool length plane at cutting speed of 280 m/min and depth of cut 0.15 mm	63
4.2.7	3D surface model in feed-tool length plane at cutting speed of 230 m/min and depth of cut 0.15 mm	63
4.4.1	Interaction Feed-Tool Length factor at CS 230 mm/min and DOC 0.15 mm. D- (22mm) D+ (52mm)	66
4.4.2	4.4.2 Cutting speed factor at depth of cut 0.15 mm feed rate of 0.12 mm/rev and tool length 37 mm	67
4.5	Tool wear classification according to Metalcutting Technical Guide	68
4.6	Chip form classification. Adapted from ISO 3685:1993	76

LIST OF ABBREVIATIONS AND SYMBOLS

D, d	-	Diameter
γ	-	Rake Angle
CS	-	Cutting Speed
DOC	-	Depth of Cut
f	-	Feed Rate
l	-	Tool Overhang Length
Ra	-	Mean Roughness
Ry	-	Maximum Peak
Rz	-	Ten-point Mean Roughness
Sm	-	Mean Spacing
t_m	-	Machining times
ANOVA	-	Analysis of Variance
RPM	-	Revolution per Minutes
DOE	-	Design of Experiment
RSM	-	Response Surface Methodology
α	-	Significance Level
CCD	-	Central Composite Design

LIST OF APPENDICES

APPENDIX	TITLE	PAGE
A	Research Schedule	87
B	Data of Chip Formation, Tool Wear and Surface Roughness	88
C	Tools & Inserts, Material, and Equipments used in Experiment	95

CHAPTER 1

INTRODUCTION

1.1 Overview

The advancement of the turning and subsequent modern technologies was made possible through research leading to the development of optimization tables that list specific feed rates, spindle speeds, and depths of cut for different materials. These tables are the standard used in industry as a source of reference, when making a change from one job to another where the machining parameters of each may be quite different. The time, material, and tooling costs associated with the experimental steps needed to find the appropriate machining parameters to eliminate for each new job, giving the company the advantage of a reduction in setup costs and to improved product quality.

In machining of parts, surface quality is one of the most specified customer requirements. There are many parameters such as cutting speed, feed rate, and tool nose radius that are known to have a large impact on surface quality. However, there are many more parameters that have an effect on the surface roughness, but those effects have not been adequately quantified. In order for manufacturers to maximize their gains, an accurate model must be constructed of the process. Several different

statistical modeling techniques have been used to generate models, including regression, surface response generation, and Taguchi methods. Though many attempts have been made to generate a model, these current models only describe a small subset of the overall process. Future work is still required to create a model that generates an accurate prediction of surface quality and gives manufacturers a robust, efficient machining process.

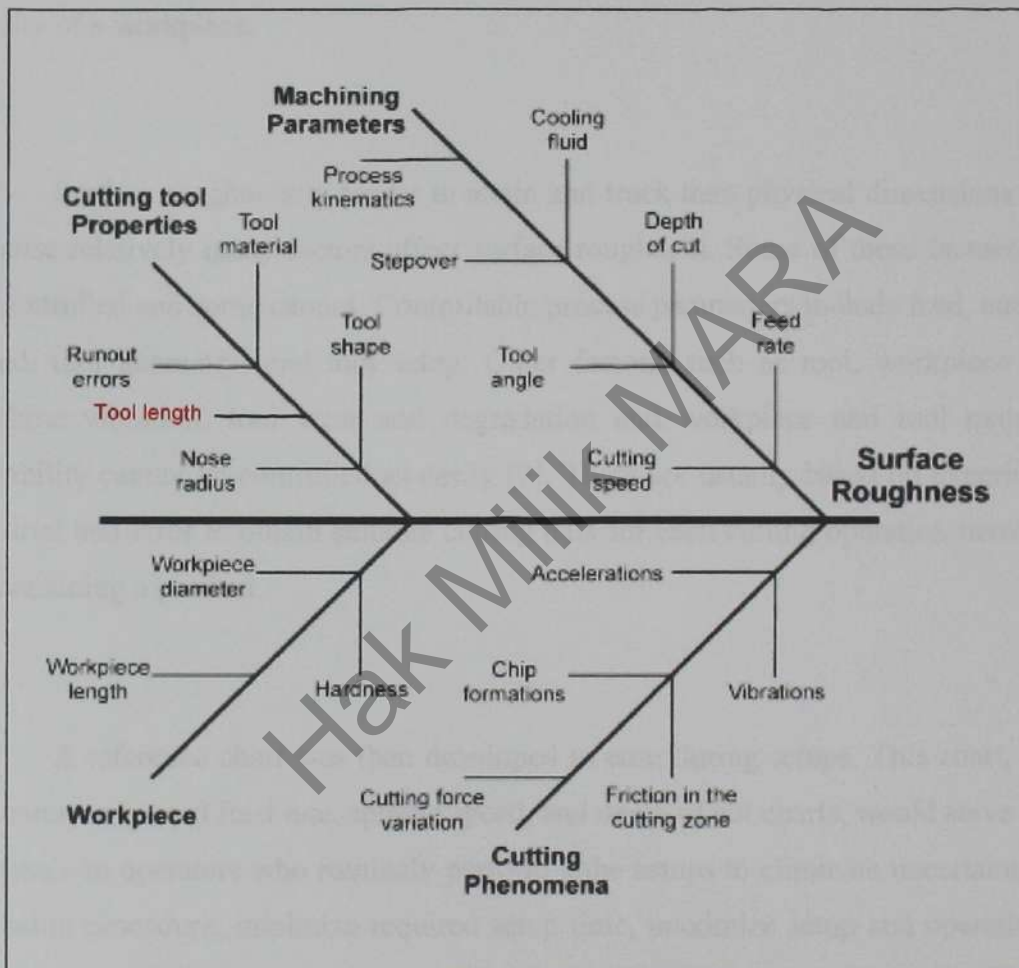


Figure 1.1 Fishbone diagram with factors that influence on surface roughness

1.2 Background and Rationale

The quality of machined components is evaluated by how closely they adhere to set product specifications of length, width, diameter, surface finish, and reflective properties. High speed turning operations, dimensional accuracy, tool wear, and quality of surface finish are three factors that manufacturers must be able to control [1]. Among various process conditions, surface finish is central to determining the quality of a workpiece.

Surface roughness is harder to attain and track than physical dimensions are, because relatively many factors affect surface roughness. Some of these factors can be controlled and some cannot. Controllable process parameters include feed, cutting speed, tool geometry, and tool setup. Other factors, such as tool, workpiece and machine vibration, tool wear and degradation and workpiece and tool material variability cannot be controlled as easily [2]. There are usually based on experience and trial and error to obtain suitable cutting data for each cutting operation involved in machining a product.

A reference chart was then developed to ease during setups. This chart, like the commonly used feed rate, spindle speed, and depth of cut charts, would serve as a reference to operators who routinely perform lathe setups to eliminate uncertainty in the setup procedure, minimize required setup time, maximize setup and operational efficiency, and reduce overall operating costs. While there are many machining optimization parameters that have been developed and put into tables, an area that has been overlooked is that of correlation between the cutting tool length and the resultant surface roughness. Thus, the choice of optimized cutting parameters becomes very important to control the required surface quality.

The aim of this research is to investigate the effects of varying cutting tool length on the resulting surface roughness in the dry turning operation of aluminum

alloy 6061. To achieve such objective, the research should have completed an experimental design that allows considering different level interactions between the cutting parameters (cutting speed, feed rate, depth of cut and tool length) on the dependant variable, surface roughness.

1.2.1 Research Objective

The objective of this study is to evaluate the effect of different cutting tool length on turning performance. A mathematical model for predicting the surface roughness will be developed. Finally the optimum cutting condition will also be proposed. After performing a cutting process, each cutting point (insert) and chip formation are check to see the appearance and condition on the surface cutting point and chip formation for each cutting condition setup by using optical microscope. The data will be compared and analyze (in term of type tool wear and chip form) for each cutting condition setup.

1.3 Research Problem

1.3.1 Statement of Research Problem

How the cutting tool length will affects the surface roughness of machined workpiece produced in turning operation.

1.3.2 Research Questions

1. What is ideal length for cutting tool to produce a good surface finish?
2. How the length of cutting tool affects the surface finish of workpiece?

1.4 Dependent and Independent Variable

The experiment was conducted using work piece material namely Aluminum Alloy 6061. This particular material, while not representative of all workpiece materials, was chosen specifically because of its widespread use in industry, and because it would be beyond the scope of this research to involve all materials at this level. The material was a standard 60 mm diameter machined bar. The bar stock consisted of several individual pieces, each being 90 mm length. The additional 25 mm in length allowed for chucking of the bar stock. The different bar lengths, were tested by machining at different tool length and then measured for surface roughness. Dry turning process is use. The independent variables for the procedures are cutting speed, feed rate, depth of cut, and tool length. The tool length variable is introduced because to investigate that the vibration generated by varying the tool length could affect the resulting surface finish. The dependent variable for the procedure is surface roughness.

1.5 Scope of Study

The scopes of thesis study are as follows:

1. Performance will be evaluated primarily in terms of surface roughness and chip form together with initial tool wear will also briefly discuss.
2. A aluminium alloy 6061 will be used as the workpiece material
3. A 20 X 20 cutting tool holder with carbide insert will be used as cutting material
4. Cutting speed, feed rate, depth of cut and tool length will be used as cutting parameters.
5. Design of Experiments techniques will be used.

1.6 Organization of Project Report

This project report is made up of five main chapters namely Introduction for Chapter 1, Literature Review for Chapter 2, Methodology for Chapter 3, Result and Discussion for Chapter 4, and lastly Conclusion for Chapter 5. First chapter describes an overview of the study and objectives that influences the study. Chapter 2 is organized to summarize the literature reviews of the relevant topic and previous work in this field to give a clear picture and guidance towards achieving the objective. In Chapter 3 describe the design or procedural plan to be followed and method to be used to conduct the study. All experiment data and result are presented in Chapter 4. In this chapter, discussions on the results are obtained and comparison will be made from previous research and theory. Finally the conclusion of study and recommendation for future work will be describes on Chapter 5.

CHAPTER 2

LITERATURE REVIEW

2.1 Introduction

The challenge of modern machining industries is mainly focused on the achievement of high quality, in terms of work piece dimensional accuracy, surface finish, high production rate, less wear on the cutting tools, economy of machining in terms of cost saving and increase the performance of the product with reduced environmental impact [3]. Surface roughness plays an important role in many areas and is a factor of great importance in the evaluation of machining accuracy [4]. Recent research that has identified the relationship between surface roughness and lesser understood turning parameters include; surface roughness versus lubrication and bed material [5], surface roughness versus tool wear [6], surface roughness versus burnishing feed rate, force, and speed [7], and surface roughness versus dry turning [8]. A regressing relationship between dimensional tolerance and workpiece length [9], and differentiate the surface roughness correlation between a supported and unsupported workpiece in relation to its length [10]. The practice of choosing appropriate process parameters can be quite difficult. To make this determination currently requires time consuming trial and error experimentation which is costly in time and material resources. The solution to this dilemma is to develop a chart to serve as a quick reference for industry to determine pre-chatter conditions, so poor

surface roughness can be avoided [11]. Cutting condition values could be put in a formula to evaluate whether the cutting conditions would produce a chatter-free workpiece. Work in this area has already begun with the development of a knowledge-based system for the prediction of surface roughness in turning process [12]. This would eliminate guesswork by optimizing cutting parameters and controlling the quality required for desired surface finishes.

A Design of Experiment (DOE) has been implemented to select manufacturing process parameters that could result in a better quality product. The DOE is an effective approach to optimize the throughput in various manufacturing-related processes [13].

2.2 Single Point Machining

2.2.1 Introduction

Turning, basically, generates cylindrical forms with a single point tool and in most cases the tool is stationary with the workpiece rotating. In many respects it is the most straight forward metal cutting method with relatively uncomplicated definitions. On the other hand, being the most widely used process and easily lending itself to development, turning today is a highly optimized process, requiring thorough appraisal of the various factors in applications. In spite of generally being a single cutting edge operation, the turning process is varied in that the workpiece shape and material, type of operation, conditions, requirements, costs, etc. determine a number of cutting tool factors. Today's turning tool is carefully designed, based on decades of experience, research and development. From the micro geometry and tool material

at its point of engagement, to the basic shape and clamping of the indexable insert through to the toolholder shank type or modular the tool handles the dynamics of metal cutting today in a way which would have been unthinkable a couple of decades ago. Many of the principles that apply to single-point machining apply also to other metal cutting methods, such as boring and even multi-point, rotating tool machining such as milling. There are several basic types of turning operations, requiring specific types of tools for the operation to be performed in the most efficient way.

Turning is the combination of two movements: rotation of the workpiece and feed movement of the tool. In some applications, the workpiece can be stationary with the tool revolving around it to make the cut, but basically the principle is the same. The feed movement of the tool can be along the axis of the workpiece, which means the diameter of the part will be turned down to a smaller size. Alternatively, the tool can be fed towards the centre (facing off), at the end of the part. Often feeds are combinations of these two directions, resulting in tapered or curved surfaces which today's CNC-turning control-units, with their many program possibilities, are able to more than cope with. This part will deal mainly with external turning, leaving other, more specialized operations, such as threading, grooving, cutting off and boring to be discussed in separate application chapters.

2.2.2 Cutting data

The workpiece rotates in the turning, with a certain spindle speed (n), at a certain number of revolutions per minute. In relation to the diameter of the workpiece, at the point it is being machined, this will give rise to a cutting speed, or surface speed (V_c) in m/min. This is the speed at which the cutting edge machines the surface of the workpiece and it is the speed at which the periphery of the cut diameter passes the cutting edge.

The cutting speed is only constant for as long as the spindle speed and/or part diameter remains the same. In a facing operation, where the tool is fed in towards the centre, the cutting speed will change progressively if the workpiece rotates at a fixed spindle speed. On most modern CNC turnings, the spindle speed is increased as the tool moves in towards the centre. For some of the cut, this makes up for the decreasing diameter but for very small diameters, and very close to the centre, this compensation will be impractical as the speed range on machines is limited. Also if a workpiece, as is often the case, has different diameters or is tapered or curved, the cutting speed should be taken into account along the variations. The feed (f_n) in mm/rev is the movement of the tool in relation to the revolving workpiece. This is a key value in determining the quality of the surface being machined and for ensuring that the chip formation is within the scope of the tool geometry. This value influences, not only how thick the chip is, but also how the chip forms against the insert geometry.

The cutting depth (a_p) in mm is the difference between uncut and cut surface. It is half of the difference between the uncut and cut diameter of the workpiece. The cutting depth is always measured at right angles to the feed direction of the tool. The cutting edge approach to the workpiece is expressed through the entering angle (κ_r). This is the angle between the cutting edge and the direction of feed and is an important angle in the basic selection of a turning tool for an operation. In addition to influencing the chip formation, it affects factors such as the direction of forces involved, the length of cutting edge engaged in cut, the way in which the cutting edge makes contact with the workpiece and the variation of cuts that can be taken with the tool in question. The entering angle usually varies between 45 to 95 degrees but for profiling operations, even larger entering angles are useful. The entering angle can be selected for accessibility and to enable the tool to machine in several feed directions, giving versatility and reducing the number of tools needed. Alternatively it can be made to provide the cutting edge with a larger corner and can add cutting edge strength by distributing machining pressure along a greater length of the cutting edge. It can also give strength to the tool at entry and exit of cut and it can direct forces to provide stability during the cut.

The cutting action is to a great extent determined by the tool geometry. The tool geometry is designed to cut various workpiece metals by forming chips in a smooth way, while also providing a strong cutting edge, and to break chips into manageable swarf. Many indexable inserts have combinations of chipbreaking functions to cope with light cuts at the corner and larger depths of cut along the cutting edge. Each insert geometry is developed to cover an application area made up of the recommended feed and cutting depth ranges. There is a distinction in cutting edge geometry between negative and positive insert geometry. A negative insert has a wedge angle of 90 degrees seen in a cross-section of the basic shape of the cutting edge. A positive insert has an angle of less than 90 degrees. The negative insert has to be inclined negatively in the toolholder so as to provide a clearance angle tangential to the workpiece while the positive insert has this clearance built-in. The inclination angle (λ) is a measure of at what angle the insert is mounted in the toolholder.

When the insert is mounted in the toolholder, the insert geometry and inclination in the toolholder will determine the resulting cutting angle with which the cutting edge cuts. The rake angle (γ) is a measure of the edge in relation to the cut although it is often expressed through a flat insert. The rake angle of the insert itself is usually positive and varies along the cutting edge, from the nose radius along the straight cutting edge. A flat insert has a rake angle of zero degrees. The actual cutting function of the rake angle also varies along the face of the insert, back from the cutting edge, until the chip breaking function takes over the chip formation. Also the actual cutting edge of the insert is subject to various developments. The micro geometry of the cutting edge is critical as regards strength and tool wear development. Edge preparation along the transition between the edge face and the clearance face is in the form of a radius, chamfer or land and affects tool strength, power consumption, finishing ability of the tool, vibration tendency and chip formation.

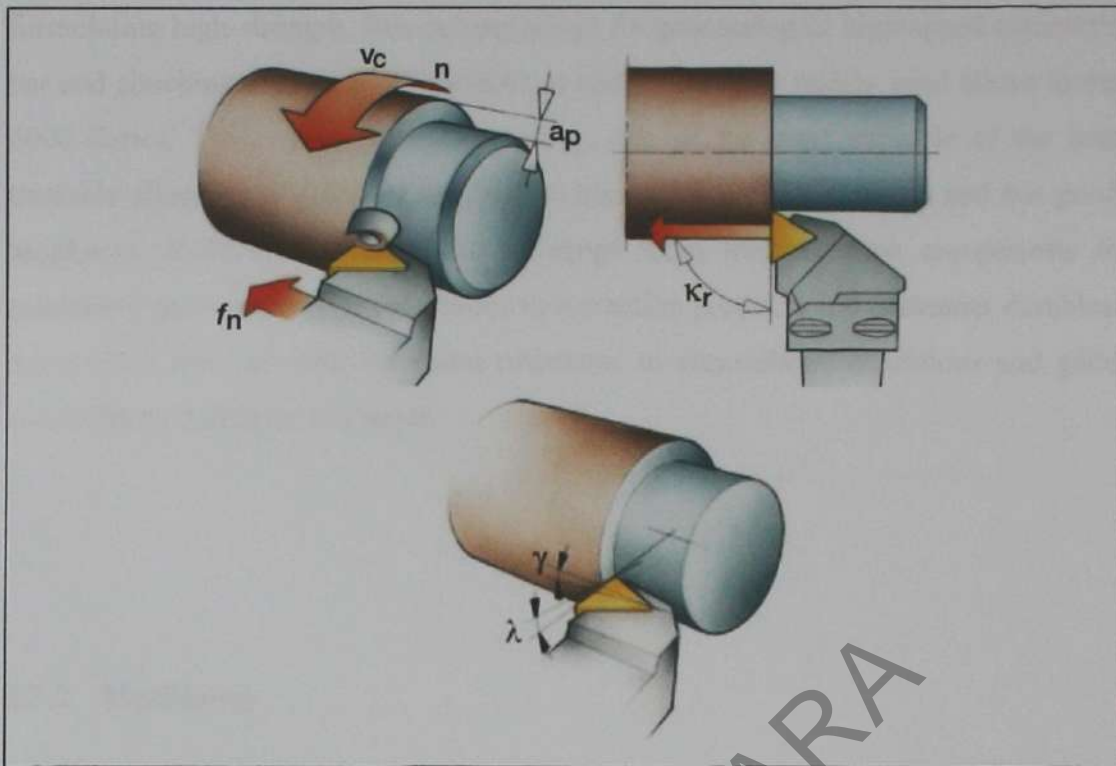


Figure 2.2.2 The main cutting data/tool elements for turning tool applications [14]

2.3 Aluminum Alloys

2.3.1 Introduction

Aluminum alloys can be machined rapidly and economically because of their complex metallurgical structure, their machining characteristics are superior those of pure aluminum. The micro constituents present in aluminum alloys have important effects on machining characteristics. Nonabrasive constituents have beneficial effects, and insoluble abrasive constituents exert a detrimental effect on tool life and surface quality. Constituents that are insoluble but soft and nonabrasive are beneficial because they assist in chip breakage; such constituents are purposely added in

formulating high-strength, free-cutting alloys for processing in high-speed automatic bar and chucking machines. Alloy 6061 is one of the most widely used alloys in the 6000 Series. This standard structural alloy, one of the most versatile of the heat treatable alloys, is popular for medium to high strength requirements and has good toughness characteristics. Applications range from transportation components to machinery and equipment applications to recreation products and consumer durables. Alloy 6061 has excellent corrosion resistance to atmospheric conditions and good corrosion resistance to sea water.

2.3.2 Machining

Alloy 6061 offers adequate machinability when machine using single point or multi spindle carbide tools on screw machines. Chips from machining may be difficult to break so chip breakers and special machining techniques (i.e. peck drilling) are recommended to improve chip formation. The alloy is rated "C" on the Aluminum Association machinability rating system, giving continuous chips and good surface finish. Extremely fine finished in the 5 to 10 micro inch range can be achieved using diamond tooling.

2.3.3 Anodizing

Alloy 6061 offers good finishing characteristics and responds well to anodizing in particular, this alloy offers excellent response to hard-coat anodizing.

2.3.4 Joining

Alloy 6061 is easily welded and joined by various commercial methods. Since 6061 is a heat treatable alloy, its strength in the -T6 condition can be reduced in the weld region. The properties listed in this Alloy Data Sheet the best current information for this alloy. In each specific application, the user is expected to evaluate and test the alloy, temper and finishing method. Consult the Material Safety Data Sheet (MSDS) for proper safety and handling precautions when using alloy 6061.

Table 2.3.4.1: 6061 Temper Designations and Definitions [15]

Standard Tempers	Standard Temper Definitions
T4, T451	Solution heat-treated and naturally aged to a substantially stable condition. Applies to products that are not cold worked after solution heat-treatment, or in which the effect of cold work in flattening or straightening may not be recognized in mechanical property limits. Temper -T451 applies to products stress-relieved by stretching.
T6, T651	Solution heat-treated and then artificially aged. Applies to products that are not cold worked after solution heat-treatment, or in which the effect of cold work in flattening or straightening may not be recognized in mechanical property limits. Temper -T651 applies to products stress-relieved by stretching.

Table 2.3.4.2: Average Coefficient of Thermal Expansion (68° to 212°F) = 13.2×10^{-6} (inch per inch per $^{\circ}\text{F}$) [15]

% Weight	Elements								Others	Others	
	Si	Fe	Cu	Mn	Mg	Cr	Zn	Ti	Each	Total	
Minimum	.40	-	.15	-	.8	.04	-	-	-	-	Aluminum
Maximum	.8	.7	.40	.15	1.2	.35	.25	.15	.05	.15	Remainder

Table 2.3.4.3: Alloy 6061 Capabilities and Mechanical Property Limits [15]

Temper	Specified Section or Wall Thickness (inches)	Tensile Strength (ksi)		Elongation	Typical Brinell Hard-ness (500 kg load/10 mm ball)	Typical ultimate Shearing Strength (ksi)	Typical Electrical Conductivity (%IACS)
		Ultimate	Yield (0.2% offset)				
		Min.	Min.	% min. in 2 inch or 4D			
Standard Tempers							
T4, T451	Up thru 8.000	30.0	16.0	18	65	24	40
T6, T651	Up thru 8.000	42.0	35.0	10	95	30	43

Hak Milik MARA

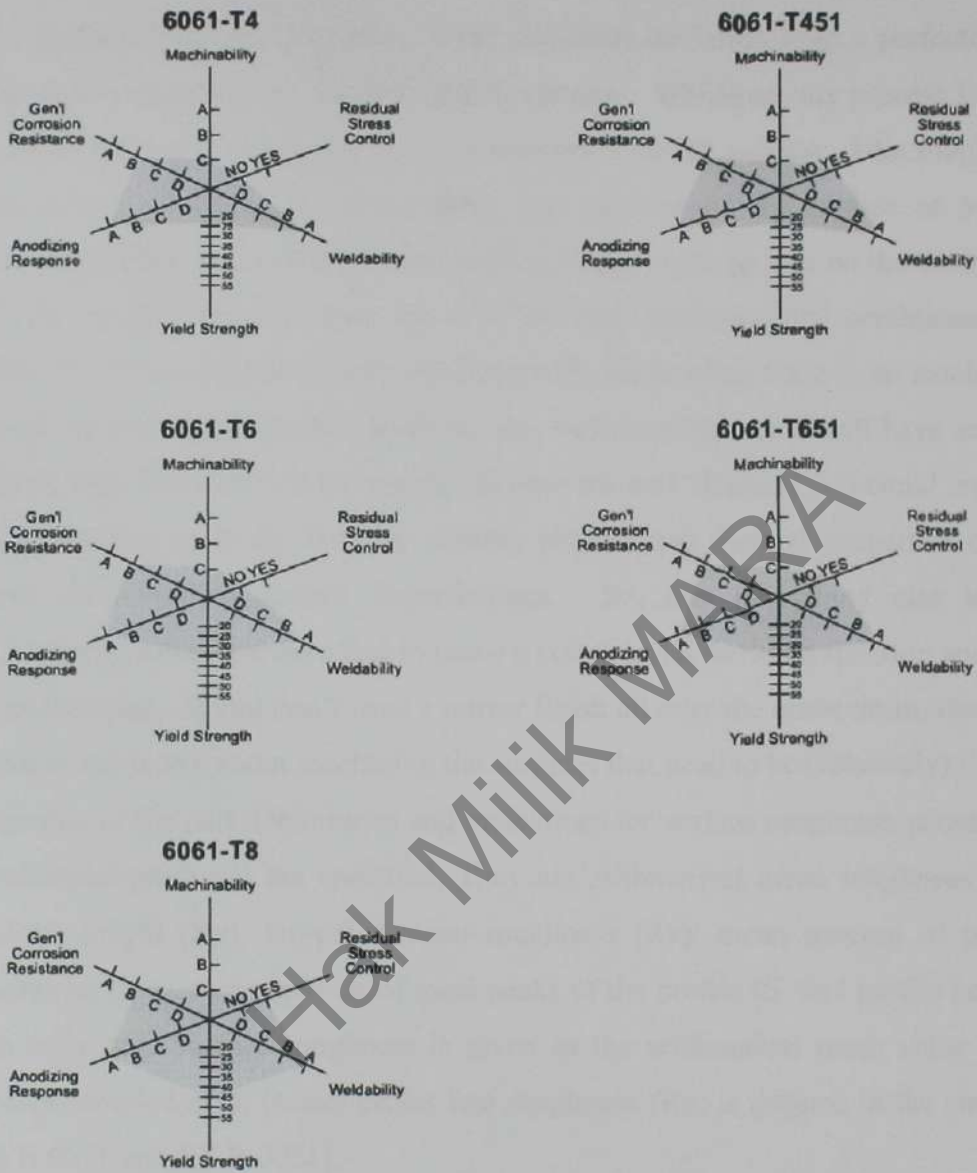


Figure 2.3.4 Comparative Characteristics of Related Alloys/Tempers [15]

2.4 Surface Roughness

Surface finish, by definition, is the allowable deviation from a perfectly flat surface that is made by some manufacturing process. Whenever any process is used to manufacture a part, there will be some roughness on the surface. This roughness can be caused by a cutting tool making tiny grooves on the surface or by the individual grains of the grinding wheel each cutting its own groove on the surface. It is affected by the choice of tool, speed of the tool, environmental conditions, and definitely by what material you are working with. Even when there is no machining involved, as in casting/injection molding, the surface of the mold will have surface deviation, which in turn will be transferred onto the part. Even if you could create a mold which was perfectly flat, the cooling process and thermal properties of the material would cause surface imperfections. So, like everything else in the manufacturing world, we have had to make a compromise between function and cost of manufacturing. If you don't need a mirror finish all over the brake drum, then you just cast it and worry about machining the surfaces that need to be (relatively) flat for the function of the part. Definitions and indications for surface roughness parameters (for industrial products) are specified. They are arithmetical mean roughness (R_a), maximum height (R_y), ten-point mean roughness (R_z), mean spacing of profile irregularities (S_m), mean spacing of local peaks of the profile (S) and profile bearing length ratio (t_p). Surface roughness is given as the arithmetical mean value for a randomly sampled area. [Mean center line roughness (R_a) is defined in the annexes of JIS B 0031 and JIS B 0061].

2.4.1 Arithmetical Mean Roughness (R_a)

A section of standard length is sampled from the mean line on the roughness chart. The mean line is laid on a Cartesian coordinate system wherein the mean line runs in the direction of the x-axis and magnification is the y-axis. The

value obtained with the formula on the right is expressed in micrometer (μm) when $y = f(x)$.

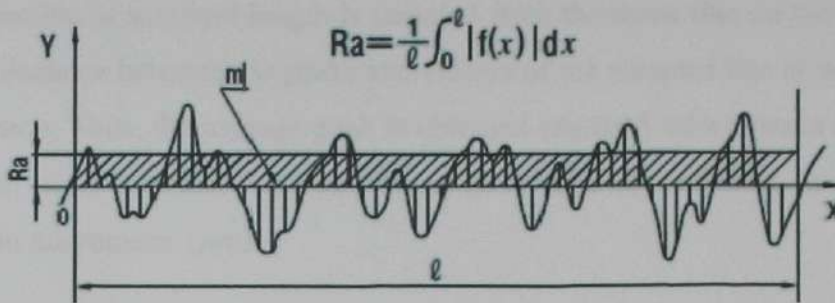


Figure 2.4.1 Arithmetical Mean Roughness (R_a) graph [16]

2.4.2 Maximum Peak (R_y)

A section of standard length is sampled from the mean line on the roughness chart. The distance between the peaks and valleys of the sampled line is measured in the y direction. The value is expressed in micrometer (μm).

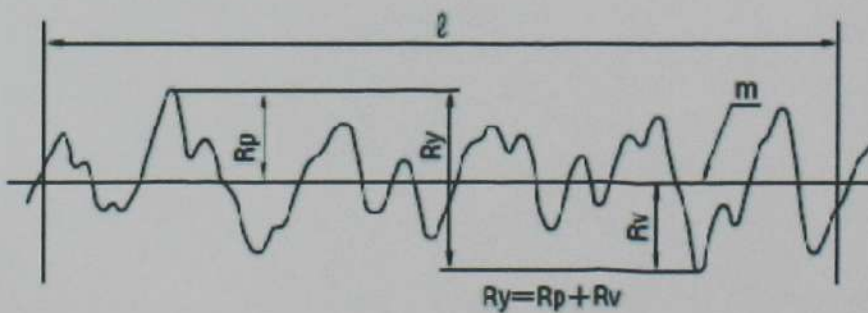
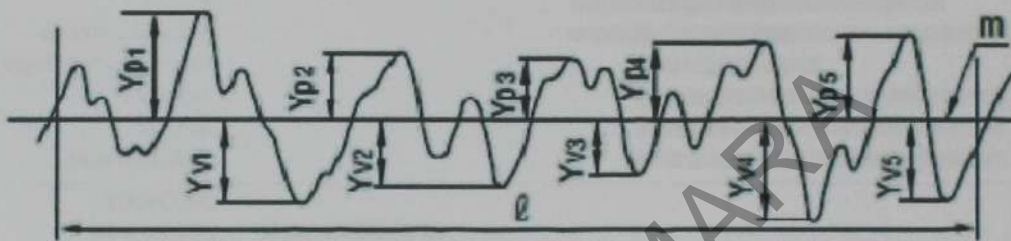


Figure 2.4.2 Maximum Peak (R_y) graph [16]

2.4.3 Ten-point Mean Roughness (R_z)

A section of standard length is sampled from the mean line on the roughness chart. The distance between the peaks and valleys of the sampled line is measured in the y direction. Then, the average peak is obtained among 5 tallest peaks (Y_p), as is the average valley between 5 lowest valleys (Y_v). The sum of these two values is expressed in micrometer (μm).



$$R_z = \frac{|Y_{p1} + Y_{p2} + Y_{p3} + Y_{p4} + Y_{p5}| + |Y_{v1} + Y_{v2} + Y_{v3} + Y_{v4} + Y_{v5}|}{5}$$

$Y_{p1}, Y_{p2}, Y_{p3}, Y_{p4}, Y_{p5}$: Tallest 5 peaks within sample

$Y_{v1}, Y_{v2}, Y_{v3}, Y_{v4}, Y_{v5}$: Lowest 5 peaks within sample

Figure 2.4.3 Ten-point Mean Roughness (R_z) graph [16]

2.5 Process Design and Improvement with Designed Experiments

2.5.1 Introduction

Quality and productivity improvement are most effective when they are an integral part of the product realization process. In particular, the formal introduction of experimental design methodology at the earliest stage of the development cycle, where new products are designed, existing product designs improved, and manufacturing processes optimized, is often the key to overall product success. The effective use of sound statistical experimental design methodology can lead to products that are easier to manufacture, have higher reliability, and have enhanced field performance. Experimental design can also greatly enhance process development and troubleshooting activities.

A designed experiment is a test or series of tests in which purposeful changes are made to the input variables of a process so that we may observe and identify corresponding changes in the output response. The process, as shown in Figure 2.5.1, can be visualized as some combination of machines, methods, and people that transforms an input material into an output product.

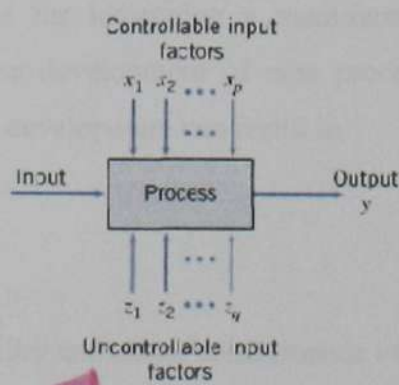


Figure 2.5.1 General model of a process [18]

This output product has one or more observable quality characteristics or responses. Some of the process variables x_1, x_2, \dots, x_p are controllable, whereas others z_1, z_2, \dots, z_p are uncontrollable (although they may be controllable for purposes of the test). Sometimes these uncontrollable factors are called noise factors. The objectives of the experiment may include

1. Determining which variables are most influential on the response, y
2. Determining where to set the influential x 's, so that y is near the nominal requirement
3. Determining where to set the influential x 's, so that variability in y is small
4. Determining where to set the influential x 's, so that the effects of the uncontrollable variables z are minimized

Thus, experimental design methods may be used either in process development or process troubleshooting to improve process performance or to obtain a process that is robust or insensitive to external sources of variability.

Experimental design a very powerful tools for the improvement and optimization of processes. Experimental design is an active statistical method: We will actually perform a series of tests on the process, making changes in the inputs and observing the corresponding changes in the outputs, and this will produce information that can lead to process improvement. Experimental design is a critically important engineering tool for improving a manufacturing process. It also has extensive application in the development of new processes. Application of these techniques early in process development can result in

1. Improved yield
2. Reduced variability and closer conformance to nominal
3. Reduced development time
4. Reduced overall costs

Experimental design methods can also play a major role in engineering design activities, where new products are developed and existing ones improved. Some applications of statistical experimental design in engineering design include

1. Evaluation and comparison of basic design configurations
2. Evaluation of material alternatives
3. Determination of key product design parameters that impact performance

Use of experimental design in these areas can result in improved manufacturability of the product, enhanced field performance and reliability, lower product cost, and shorter product development time.

2.5.2 Guidelines for Designing Experiments

Designed experiments are a powerful approach to improving a process. To use this approach, it is necessary have a clear idea in advance of the objective of the experiment, exactly what factors are to be studied, how the experiment is to be conducted, and at least a qualitative understanding of how the data will be analyzed. Montgomery gives an outline of the recommended procedure

- | | | | | |
|------------------------------|---|--|---|--|
| Pre-experimental
planning | [| 1. Recognition of and statement of the problem |] | Often done
simultaneously, or
in reverse order |
| | | 2. Choice of factors and levels | | |
| | | 3. Selection of the response variable | | |
| | | 4. Choice of experimental design | | |
| | | 5. Performing the experiment | | |
| | | 6. Data analysis | | |
| | | 7. Conclusion and recommendations | | |

2.5.3 Factorial Experiments

When there are several factors of interest in an experiment, a factorial design should be used. In such designs factors are varied together. Specifically, by a factorial experiment we mean that in each complete trial or replicate of the experiment all possible combinations of the levels of the factors are investigated. Thus, there are three factors A , B and C ($k=3$), this design has eight factor level combinations. Geometrically, the design is a cube as shown in Figure 2.5.3.1(a), with the eight run forming the corners of the cube. Figure 2.5.3.1(b) shows the test matrix.

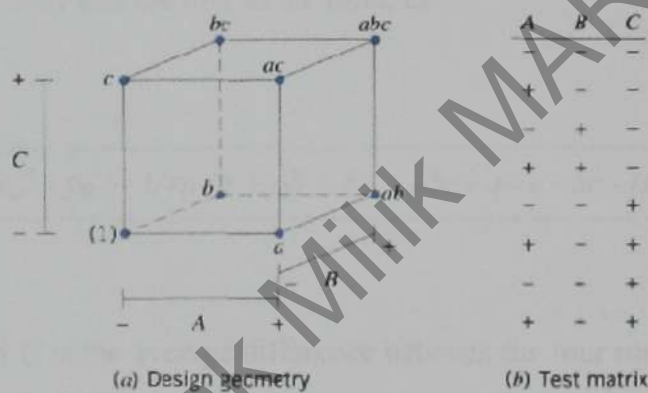


Figure 2.5.3.1 The 2^3 factorial design [18]

This design allows three main effects to be estimated (A , B , and C) along with three two-factor interactions (AB , AC , and BC) and a three-factor interaction (ABC). Thus, the full factorial model could be written symbolically as

$$y = \mu + A + B + C + AB + AC + BC + ABC + \varepsilon$$

where μ is an overall mean, ε is a random error term assumed to be $NID(0, \sigma^2)$, and the uppercase letters represent the main effects and interactions of the factors. The

main effects can be estimated easily. The lowercase letters (1), a , b , ab , c , ac , bc , and abc represent the total of all n replicates at each of the eight runs in the design. Referring to the cube in Figure 2.5.3.1, we would estimate the main effect of A by averaging the four runs on the right side of the cube where A is at the high level and subtracting from that quantity the average of the four runs on the left side of the cube where A is at the low level. This gives

$$A = \bar{y}_A^+ - \bar{y}_A^- = 1/4n [a + ab + ac + abc - b - c - bc - (1)] \dots (1)$$

In a similar manner, the effect of B is the average difference of the four runs in the back face of the cube and the four in the front, or

$$B = \bar{y}_B^+ - \bar{y}_B^- = 1/4n [b + ab + bc + abc - a - c - ac - (1)] \dots (2)$$

and the effect of C is the average difference between the four runs in the top face of the cube and the four in the bottom, or

$$C = \bar{y}_C^+ - \bar{y}_C^- = 1/4n [c + ac + bc + abc - a - b - ab - (1)] \dots (3)$$

The top row of Figure 2.5.3.2 shows how the main effects of the three factors are computed. Now consider the two-factor interaction AB . When C is at the low level, AB is simply the average difference in the A effect at the two levels of B , or

$$AB(C \text{ low}) = 1/2n [ab - b] - 1/2n [a - (1)]$$

Similarly, when C is at the high level, the AB interaction is

$$AB(C \text{ high}) = 1/2n [abc - bc] - 1/2n [ac - c]$$

The AB interaction is the average of these two components, or

$$A = 1/4n [ab + (1) + abc + c - b - a - bc - ac] \dots (4)$$

Note that the AB interaction is simply the difference in averages on two diagonal planes in the cube (refer to the left-most cube in the middle row of Figure 2.5.3.2).

Using a similar approach, we see from the middle row of Figure 2.5.3.2 that the AC and EC interaction effect estimates are as follows:

$$AC = 1/4n [ac + (1) + abc + b - a - c - ab - bc] \dots (5)$$

$$BC = 1/4n [bc + (1) + abc + a - b - c - ab - ac] \dots (6)$$

The ABC interaction effect is the average difference between the AB interactions at the two levels of C . Thus

$$ABC = 1/4n \{ [abc - bc] - [ac - c] - [ab - b] + [a - (1)] \}$$

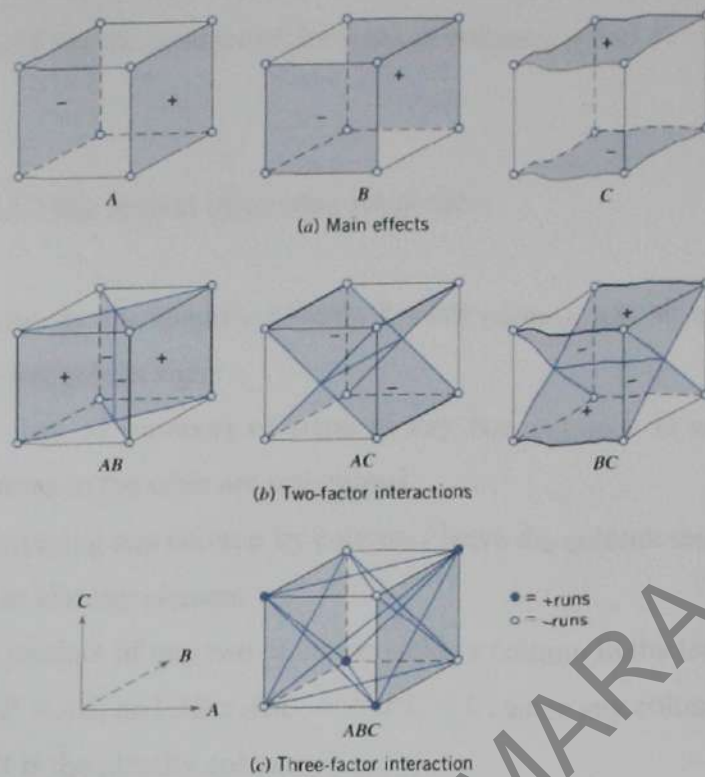


Figure 2.5.3.2 Geometric presentation of contrasts corresponding to the main effects and interaction in the 2^3 design [18]

or

$$ABC = 1/4n [abc - bc - ac + c - ab + b + a - (1)] \dots (7)$$

This effect estimate is illustrated in the bottom row of Figure 2.5.3.2.

The quantities in brackets in equations 1 through 7 are contrasts in the eight factor-level combinations. These contrasts can be obtained from a table of plus and minus signs for the 2^3 design. Signs for the main effects (columns A , B , and C) are obtained by associating a plus with the high level and a minus with the low level. Once the signs for the main effects have been established, the signs for the remaining columns are found by multiplying the

appropriate preceding columns, row by row. For example, the signs in column AB are the product of the signs in columns A and B .

Table 2.5.3 has several interesting properties:

1. Except for the identity column I , each column has an equal number of plus and minus signs
2. The sum of products of signs in any two columns is zero; that is, the columns in the table are orthogonal
3. Multiplying any column by column I leave the column unchanged; that is, I is an identity element
4. The product of any two columns yields a column in the table; for example, $A \times B = AB$, and $AB \times ABC = A^2B^2C = C$, since any column multiplied by itself is the identity column

Table 2.5.3: Signs for effects in the 2^3 design

Treatment combination	Factorial Effect							
	I	A	B	AB	C	AC	BC	ABC
(I)	+	-	-	+	-	+	+	-
a	+	+	-	-	-	-	+	+
b	+	-	+	-	-	+	-	+
ab	+	+	+	+	-	-	-	-
c	+	-	-	+	+	-	-	+
ac	+	+	-	-	+	+	-	-
bc	+	-	+	-	+	-	+	-
abc	+	+	+	+	+	+	+	+

The estimate of any main effect or interaction is determined by multiplying the factor level combinations in the first column of the table by the signs in the corresponding main effect or interaction column, adding the

result to produce a contrast, and then dividing the contrast by one-half the total number of runs in the experiment. Expressed mathematically,

$$\text{Effect} = \text{Contrast} / n2^{k-1} \dots (8)$$

The sum of squares for any effect is

$$SS = (\text{Contrast})^2 / n2^k \dots (9)$$

2.6 Process Optimization with Designed Experiment

2.6.1 Introduction

Once the appropriate subset of process variables are identified, the next step is usually process optimization, or finding the set of operating conditions for the process variables that result in the best process performance. This is probably the most widely used and successful optimization technique based on designed experiments. These are activities in which process engineering personnel try to reduce the variability in the output of a process by setting controllable factors to levels that minimize the variability transmitted into the responses of interest by other factors that are difficult to control during routine operation.

2.6.2 Response Surface Methods and Designs

Response surface methodology (RSM) is a collection of mathematical and statistical techniques that are useful for modeling and analysis in applications where a response of interest is influenced by several variables and the objective is to optimize this response.

In most RSM problems, the form of the relationship between the response and the independent variables is unknown. Thus, the first step in RSM is to find a suitable approximation for the true relationship between y and the independent variables. Usually, a low-order polynomial in some region of the independent variables is employed. If the response is well modeled by a linear function of the independent variables, then the approximating function is the *first-order model*

$$y = \beta_0 + \beta_1 x_1 + \beta_2 x_2 + \dots + \beta_k x_k + \varepsilon \dots (1)$$

If there is curvature in the system, then a polynomial of higher degree must be used, such as the *second-order model*

$$y = \beta_0 + \sum_{i=1}^k \beta_i x_i + \sum_{i=1}^k \beta_{ii} x_i^2 + \dots + \sum_{i < j=2}^k \beta_{ij} x_i x_j + \varepsilon \dots (2)$$

Many RSM problems utilize one or both of these approximating polynomials. Of course, it is unlikely that a polynomial model will be a reasonable approximation of the true functional relationship over the entire space of the independent variables, but for a relatively small region they usually work quite well.

The method of least squares is used to estimate the parameters in the approximating polynomials. That is, the estimates of the β 's in equations 1 and 2 are those values of the parameters that minimize the sum of squares of the model errors. The response surface analysis is then done in terms of the fitted surface. If the fitted surface is an adequate approximation of the true response function, then analysis of the fitted surface will be approximately equivalent to analysis of the actual system. The eventual objective of RSM is to determine the optimum operating conditions for the system or to determine a region of the factor space in which operating specifications are satisfied. Also, note that the word "optimum" in RSM is used in a special sense. The "hill climbing" procedures of RSM guarantee convergence to a local optimum only.

2.6.3 The Method of Steepest Ascent

Frequently, the initial estimate of the optimum operating conditions for the system will be far away from the actual optimum. In such circumstances, the objective of the experimenter is to move rapidly to the general vicinity of the optimum. We wish to use a simple and economically efficient experimental procedure. When we are remote from the optimum, we usually assume that a first-order model is an adequate approximation to the true surface in a small region of the x 's. The method of steepest ascent is a procedure for moving sequentially along the path of steepest ascent, that is, in the direction of the maximum increase in the response. Of course, if minimization is desired, then we would call this procedure the method of steepest descent. The fitted first-order model is

$$\hat{y} = \hat{\beta}_0 + \sum_{i=1}^k \hat{\beta}_i x_i \quad \dots (3)$$

and the first-order response surface, that is, the contours of y is a series of parallel straight lines such as shown in Figure 2.6.3. The direction of steepest ascent is the direction in which y increases most rapidly. This direction is normal to the fitted response surface contours. We usually take as the path of steepest ascent the line through the center of the region of interest and normal to the fitted surface contours. Thus, the steps along the path are proportional to the magnitudes of the regression coefficients $\{\beta_i\}$. The experimenter determines the actual amount of movement along this path based on process knowledge or other practical considerations.

Experiments are conducted along the path of steepest ascent until no further increase in response is observed or until the desired response region is reached. Then a new first-order model may be fitted, a new direction of steepest ascent determined, and, if necessary, further experiments conducted in that direction until the experimenter feels that the process is near the optimum.

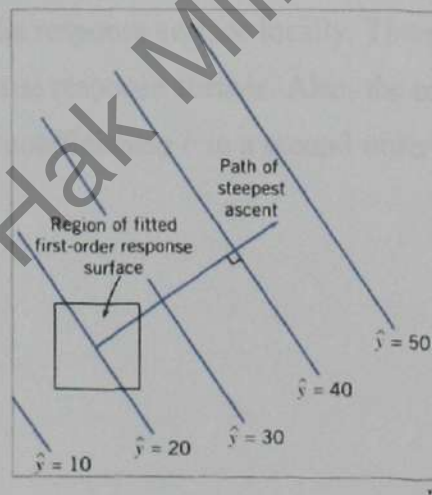


Figure 2.6.3 First order response surface and path of steepest ascent [19]

2.6.4 Analysis of a Second-Order Response Surface

When there is a curvature in the response surface the first-order model is insufficient. A second-order model is useful in approximating a portion of the true response surface with parabolic curvature.

The second-order model includes all the terms in the first-order model, plus all quadratic terms like and all cross product terms. It is usually expressed as

$$y = \beta_0 + \sum_{i=1}^k \beta_i x_i + \sum_{i=1}^k \beta_{ii} x_i^2 + \dots + \sum_{i < j=2}^k \beta_{ij} x_i x_j + \varepsilon \dots (2)$$

The second-order model is flexible, because it can take a variety of functional forms and approximates the response surface locally. Therefore, this model is usually a good estimation of the true response surface. Also, the method of least squares can be applied to estimate the coefficients β in a second-order model.

CHAPTER 3

METHODOLOGY

3.1 Introduction

An experimental design was created to test the surface roughness of varying cutting tool extension length in a straight turning process. The experiments involving two different cutting tool lengths. The surface roughness was measured for each of the test increments. The surface roughness values reflected the difference in surface finish as the cutting tool extension length is changed. Since previously published research on this specific subject is very limited, the results of the study were based on empirical evidence obtained during the course of the experiments performed during this research. This research project was designed to address the issue in a general manner, focusing on straight turning of aluminum alloy 6061 using a finishing cut. The research laboratory used is situated in the KKTM, Balik Pulau, Pulau Pinang. The equipment chosen for use in the experimental process are:

1. CNC TURNING - DMG CTX 310 GILDEMEISTER
2. EXTERNAL TOOL HOLDER - PDJNL2020-43
3. INDEXABLE INSERTS FOR TURNING - DNMG110404N-GU
4. MITUTOYO SURFACE ROUGHNESS
5. ALUMINUM ALLOY 6061

3.1.1 CNC Turning - DMG CTX 310 GILDIMEISTER

The study was carried out using a CNC Turning DMG CTX 310 Glidimiester a equipped with 45° slanted bed that is designed as a rigid 4-track bed with linear roller guide way, maximum reach of 16.5 in. and a swing diameter of 13 in. above bed; it is ideally suited for smaller and medium size work-pieces. Apart from the above mentioned control alternatives, tailstock and chip conveyor delivered as standard, it contains a 12-disk turret with 6 driven tools, a bar machining and hollow cylinder and tool probe. The technical data for CTX 310 are presented as follows:



Figure 3.1.1.1 CNC Turning DMG CTX 310 Glidimiester [20]

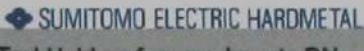
Machine Type	Unit	CTX3 10
Work area		
Swing diameter, max	mm	505
Swing diameter above cross guideway	mm	375
Cross travel (X)	mm	213/140
Vertical travel (Y)	mm	±40
Longitudinal travel (Z)	mm	450
Main spindle		
Spindle head (flat flange)	mm	140h5
Bar capacity	mm	51/65
Spindle diameter in the front bearing	mm	100
Chuck	mm	170/210
Drive power (40/100% DC)	kW (AC)	16/12
Max torque (40/100% DC)	Nm	153/115
Rotational speed range	rpm	25-6000
Feed drive AC		
Rapid traverse X / Y / Z		24 / 10 / 30
Tool mount		
No. of tool stations,		12
Powered tool stations	mm	12
Shaft diameter	mm	30
Drive power (40% DC)	kW	9 / 6.7
Tool mount		
Max torque (40% DC)	Nm	20 / 16
Max rotational speed	rpm	4500 / 4000
Max clamping diameter of the powered tools	mm	16
Tailstock		
Tailstock stroke (auto. traversable)	mm	450
Centre punch fitting	MK	4
Quill diameter / stroke	mm	-
Max tailstock power	daN	400
Machine weight with chip conveyor	kg	3500 / 3700
Controls		
DMG SlimLine Panel with 15" TFT Screen		Siemen 840D

Figure 3.1.1.2 Technical Data for CNC Turning DMG CTX 310 Glidimiester [20]

3.1.2 External Tool Holder - PDJNL2020-43


The cutting tool holder was used for this study is Sumitomo SEC-External Tool Holder with PDJN Type and left side for general turning and copying. Below show the details data for the holder:

PDJN / PDNN

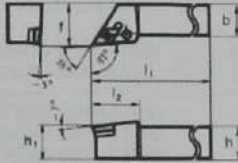


SUMITOMO ELECTRIC HARDMETAL
Tool Holders for neg. Inserts DN...


P-Type Lever-Lock Holders



PDJN








■ INSERTS



Eg.
● DNMG 110408 N-GU
● DNMM 150508 N-HG

■ SPARE PARTS

	Lever pin	Clamp bolt	Shim	Shim pin	Wrench	Insert
						

■ HOLDERS

Above figures show right-hand tools.

Ordering No.	Stock		Dimensions (mm)						Lever pin	Clamp bolt	Shim	Shim pin	Wrench	Insert	
	R	L	h	h ₁	b	l ₁	l ₂	f							
PDJN R/L 1616 H11	●	●	16	16	16	100	30	20							
PDJN R/L 2020 K11	●	●	20	20	20	125	30	25	LCL3S-SD	LC31TB-SD	LSD32SD	LSP3SD	LH025	●	
PDJN R/L 2525 M11	●	●	25	25	25	150	30	32							
PDJN R/L 2020 K15	●	●	20	20	20	125	34.7	25							
PDJN R/L 2525 M15	●	●	25	25	25	150	34.7	32							
PDJN R/L 3225 P15	●	●	32	32	25	170	34.7	32							
PDJN R/L 4025 P15			40	40	25	170	35	28.7							

External holder for neg. inserts



PDJN



Figure 3.1.2 Tool Holders for Negative Insert [21]

3.1.3 Indexable Inserts for Turning - DNMG110404N-GU

The insert chosen for this research was the DNMG110404N-GU Grade AC2000. It is a TiN coated carbide insert that is designed for general purpose machining has negative rake geometry. Its shape is diamond with 55° nose angle and a 0° relief angle. Using the SUMITOMO Performance Cutting Tools (2007~2008), which illustrates specifications for the insert:

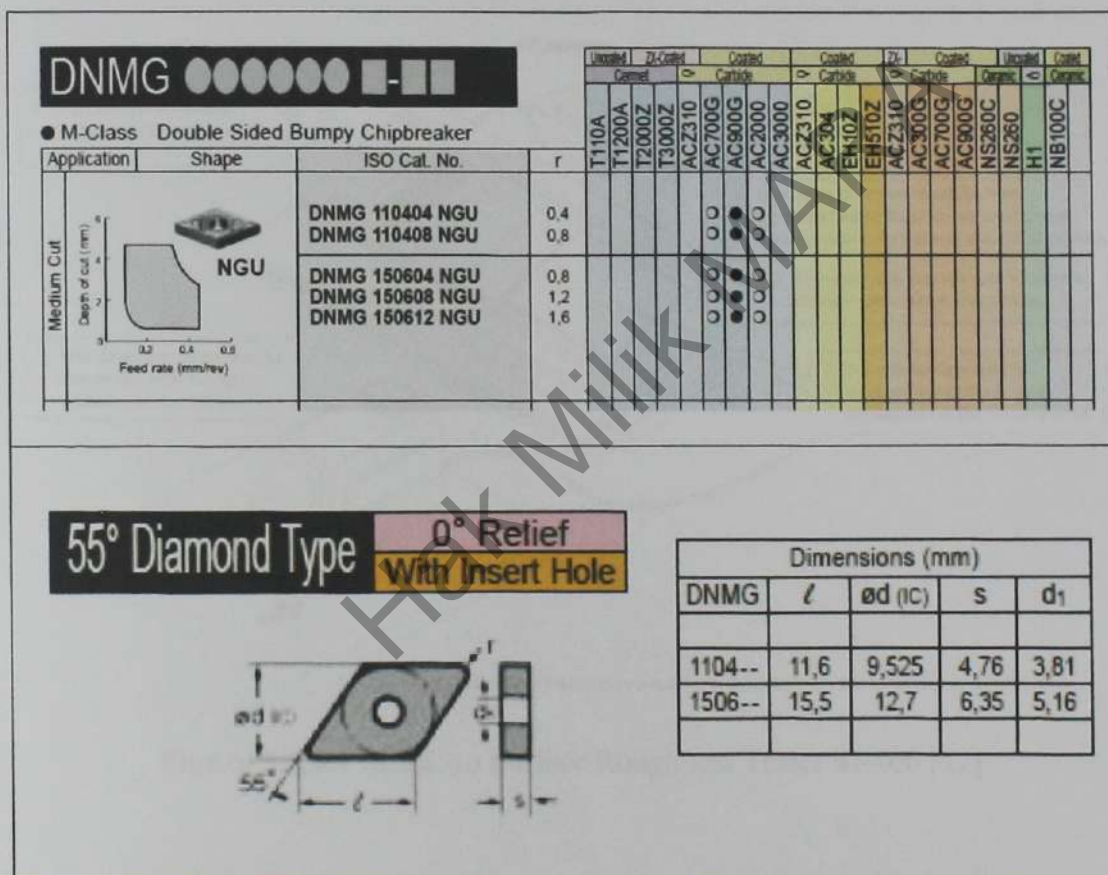


Figure 3.1.3 Indexable Inserts for Turning [21]

3.1.4 Mitutoyo Surface Roughness Tester SJ-400

The SurfTest SJ-400 is a stylus type surface roughness measuring instrument developed for shop use. The SJ-400 is capable of evaluating surface textures including waviness with a variety of parameters according to various national standards and international standards. The measurement results are displayed digitally/graphically on the touch panel, and output to the built-in printer.

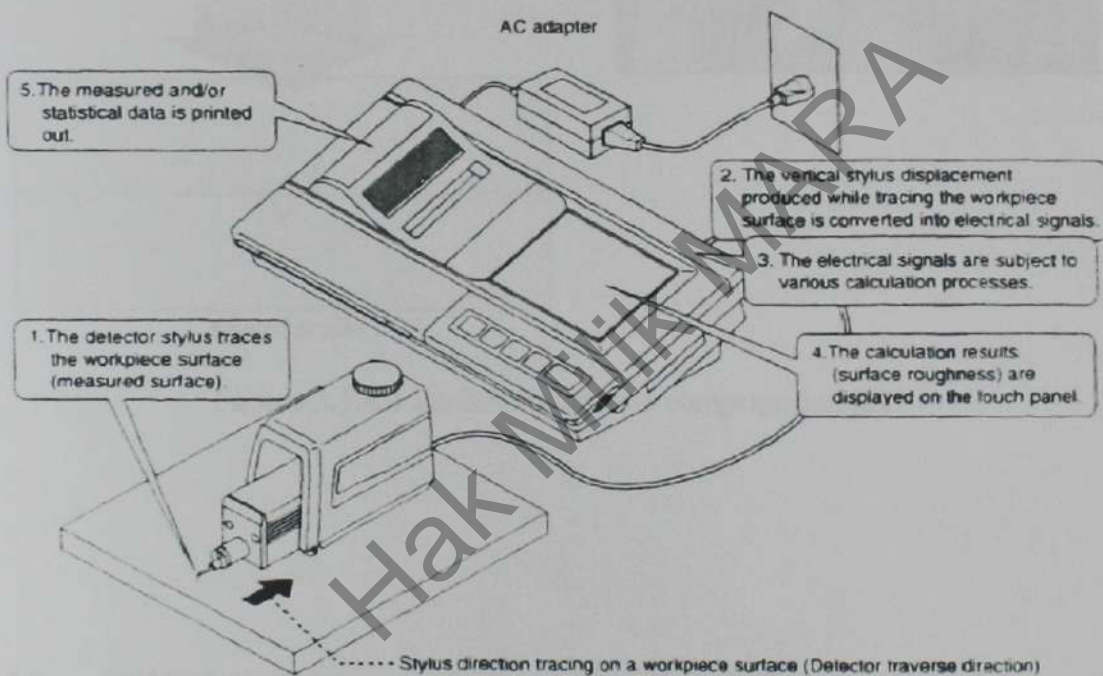


Figure 3.1.4.1 Mitutoyo Surface Roughness Tester SJ-400 [22]

The stylus of the SJ-400 detector unit traces the minute irregularities of the workpiece surface. Surface roughness is determined from the vertical stylus displacement produced during the detector traversing over the surface irregularities. The measurement results are displayed digitally/graphically on the touch panel, and output to the built-in printer.

Usually, a spherical or cylindrical surface (R-surface) cannot be evaluated, but, by removing the radius with a filter, R-surface data is processed as it taken from a flat surface.

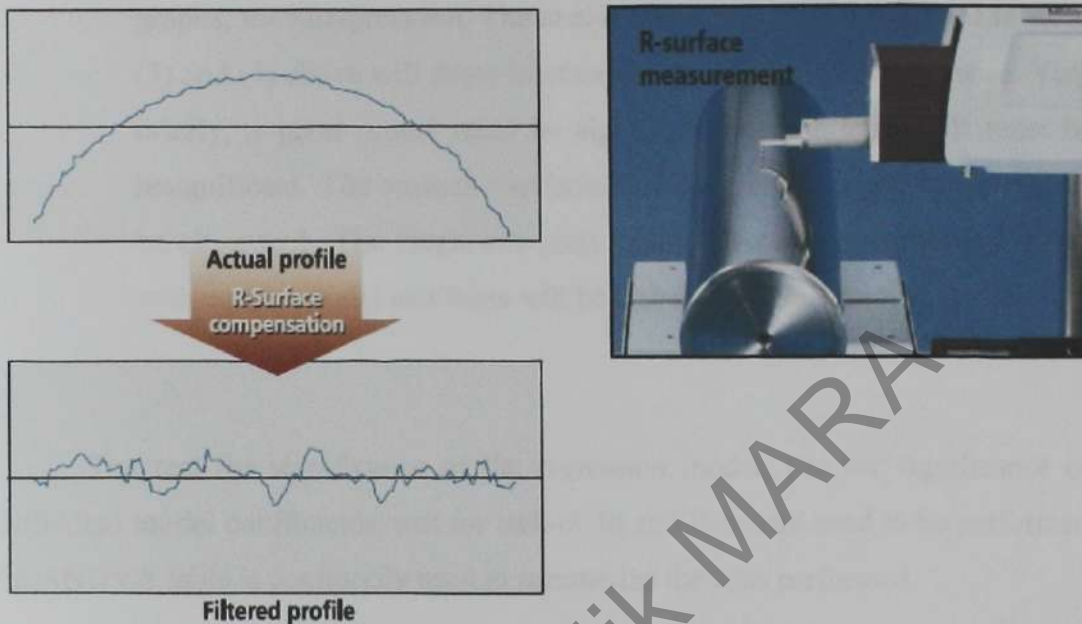


Figure 3.1.4.2 Surface Roughness compensation [22]

3.2 RSM Methodology

The version 8 of the Design Expert software was used to develop the experimental plan for RSM. The same software was also used to analyze the data collected by following the steps as follows:

1. Choose a transformation if desired. Otherwise, leave the option at "None".
2. Select the appropriate model to be used. The Fit Summary button displays the sequential F -tests, lack-of-fit tests and other adequacy measures that could be used to assist in selecting the appropriate model.

3. Perform the analysis of variance (ANOVA), post-ANOVA analysis of individual model coefficients and case statistics for analysis of residuals and outlier detection.
4. Inspect various diagnostic plots to statistically validate the model.
5. If the model looks good, generate model graphs, i.e. the contour and 3D graphs, for interpretation. The analysis and inspection performed in steps (3) and (4) above will show whether the model is good or otherwise. Very briefly, a good model must be significant and the lack-of-fit must be insignificant. The various coefficient of determination, R^2 values should be close to 1. The diagnostic plots should also exhibit trends associated with a good model and these will be elaborated subsequently.

The test for significance of the regression model, test for significance on individual model coefficients, test for lack-of-fit and R-square need to be performed. An ANOVA table is commonly used to summarize the tests performed.

3.2.1 Test for significance of the regression model

This test is performed as an ANOVA procedure by calculating the F-ratio, which is the ratio between the regression mean square and the mean square error. The F-ratio, also called the variance ratio, is the ratio of variance due to the effect of a factor (in this case the model) and variance due to the error term. This ratio is used to measure the significance of the model under investigation with respect to the variance of all the terms included in the error term at the desired significance level, α . A significant model is desired.

3.2.2 Test for significance on individual model coefficients

This test forms the basis for model optimization by adding or deleting coefficients through backward elimination, forward addition or stepwise elimination/addition/exchange. It involves the determination of the P-value or probability value, usually relating the risk of falsely rejecting a given hypothesis. For example, a "Prob. > F" value on an F-test tells the proportion of time you would expect to get the stated F-value if no factor effects are significant. The "Prob. > F" value determined can be compared with the desired probability or α -level. In general, the lowest order polynomial would be chosen to adequately describe the system.

3.2.3 Lack-of-Fit

As replicate measurements are available, a test indicating the significance of the replicate error in comparison to the model dependent error can be performed. This test splits the residual or error sum of squares into two portions, one which is due to pure error which is based on the replicate measurements and the other due to lack-of-fit based on the model performance. The test statistic for lack-of-fit is the ratio between the lack-of-fit mean square and the pure error mean square. As previously, this F-test statistic can be used to determine as to whether the lack-of-fit error is significant or otherwise at the desired significance level, α . Insignificant lack-of-fit is desired as significant lack-of-fit indicates that there might be contributions in the regressor response relationship that are not accounted for by the model.

3.2.3 R-Square

Additionally, checks need to be made in order to determine whether the model actually describes the experimental data [23]. The checks performed here include determining the various coefficient of determination, R^2 . These R^2 coefficients have values between 0 and 1. In addition to the above, the adequacy of the model is also investigated by the examination of residuals. The residuals, which are the difference between the respective, observe responses and the predicted responses are examined using the normal probability plots of the residuals and the plots of the residuals versus the predicted response. If the model is adequate, the points on the normal probability plots of the residuals should form a straight line. On the other hand the plots of the residuals versus the predicted response should be structure less, that is, they should contain no obvious patterns.

3.3 Experimental Setup

An experimental design was created to test the resultant surface roughness of varying cutting tool length in a straight turning process for finishing cutting. The experiments was conducted using workpiece material namely Aluminum alloy 6061-T41 with TiN coated carbide cutting tool manufactured by SUMITOMO. The material was a standard 60 mm diameter unmachined bar with a total length 90 mm (the material a choose in the same long unmachined bar; try to reduce a different structure of material properties that could affect the results). The additional 25 mm in length allowed for chucking of the bar stock. Chamfer with $1 \times 45^\circ$ was performed at the initial of workpiece to reduce sudden impact between cutting tool and material that may affect the result. Figure 3.3.1 show the workpiece dimensions.

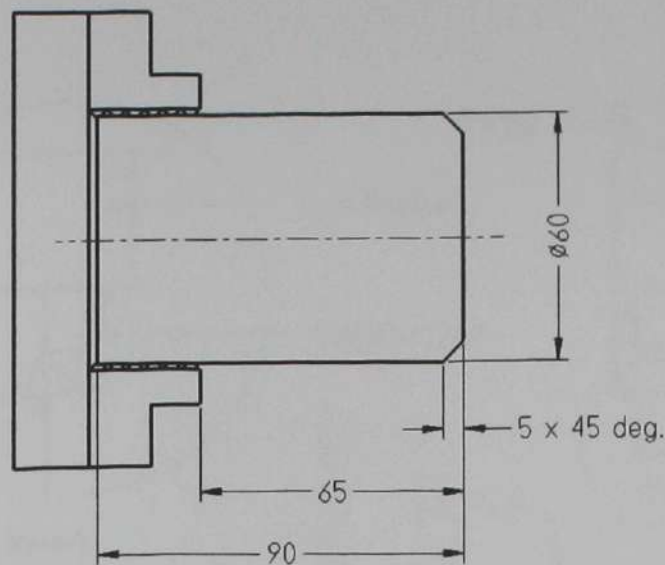


Figure 3.3.1 Illustration of workpiece dimension

This particular material, while not representative of all workpiece materials, was chosen specifically because of its widespread use in industry, and because it would be beyond the scope of this research to involve all materials at this level.

The workpiece will cut in form of external straight turning for certain length. The length of cutting is depends on the time machining. The time of machining has been set to 0.24 minutes (14.4 seconds) for each condition. This is to make sure the effects on cutting tool are at the same time. The standard cutting tool length is 129 mm (from end of tool body to insert tip) and after attach at tool holder the hanging area length is 52 mm. The cutting tool will be performed machining with hanging area at high 52 mm and low at 22 mm length and the surface roughness will be checked to determine the idle tool length with good surface roughness. Twenty-eight workpiece and twenty-eight new cutting point will use for each group cutting condition setting. Figure 3.3.2 show the experimental setting of the workpiece and the cutting tool.

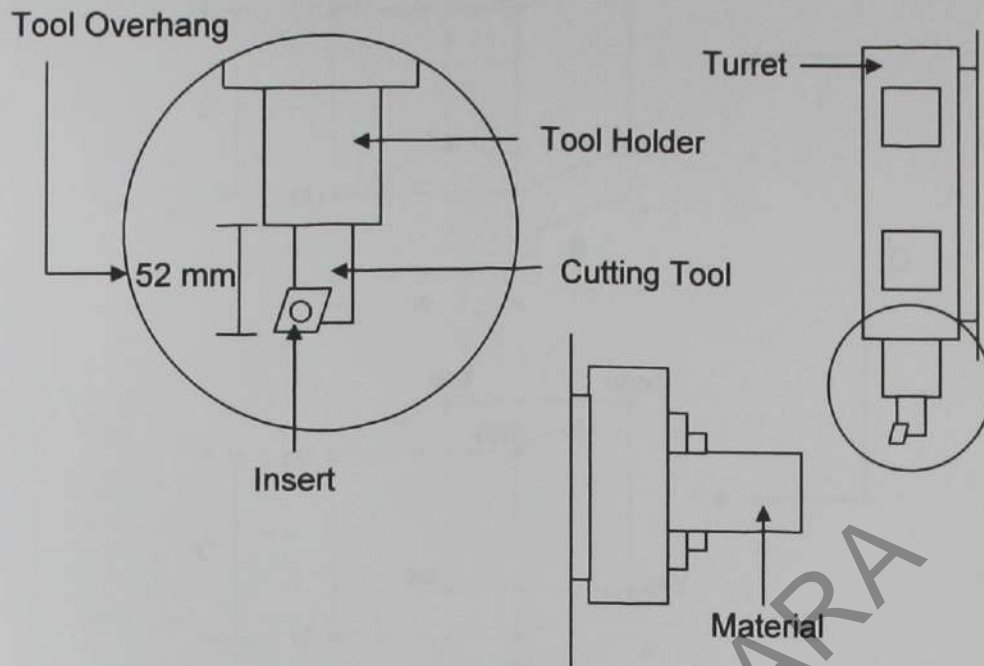


Figure 3.3.2 Experimental setup

After perform a cutting process, each cutting point (insert) and chip formation are check to see the appearance and condition on the surface cutting point and chip formation for each cutting condition setup by using optical microscope. The data will be compared and analyze with each cutting condition setup.

The experiments, involving twenty-eight (28) groups of experimental testing and results. The experiment is a 2^4 factorial design in the factors cutting speed (A), feed rate (B), depth of cut tool angle (C), and tool overhang (D). Geometrically, the design is a cube as shown in Figure 3.3.3, with sixteen run forming the corners of the cube, replicates of factorial is 1, replicates of axial (star) point is 1 and center point is 4. Table 3.3.1 shows the test matrix.

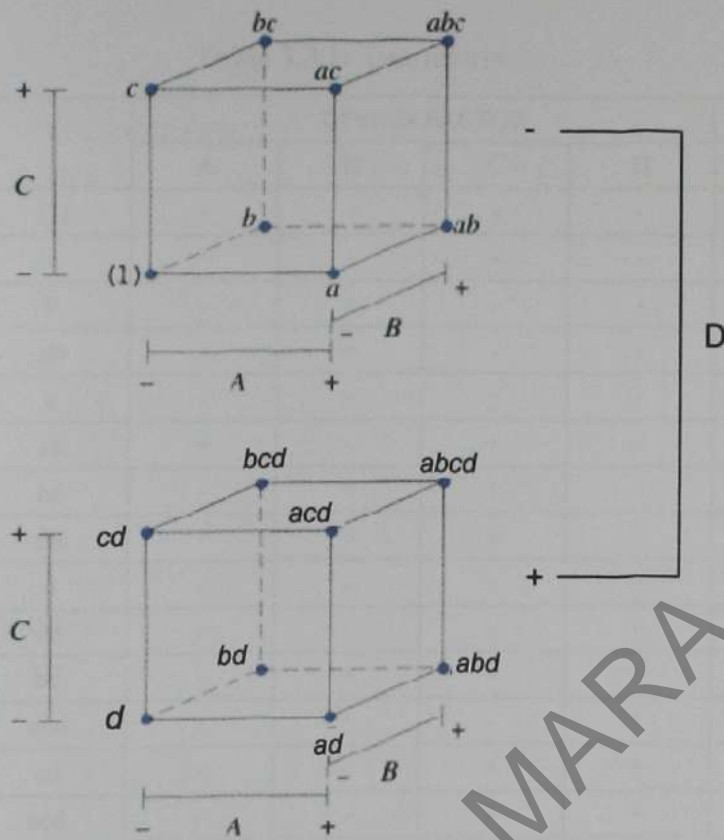


Figure 3.3.3 Factorial 2⁴ design for the surface finish experiment [18]

Hak Milk MARA

Table 3.3.1: Test matrix

NO		DESIGN FACTOR				Ra
		A	B	C	D	
1	(I)	-	-	-	-	
2	a	+	-	-	-	
3	b	-	+	-	-	
4	ab	+	+	-	-	
5	c	-	-	+	-	
6	ac	+	-	+	-	
7	bc	-	+	+	-	
8	abc	+	+	+	-	
9	d	-	-	-	+	
10	ad	+	-	-	+	
11	bd	-	+	-	+	
12	abd	+	+	-	+	
13	cd	-	-	+	+	
14	acd	+	-	+	+	
15	bcd	-	+	+	+	
16	abcd	+	+	+	+	
17	axial	-	0	0	0	
18	axial	+	0	0	0	
19	axial	0	-	0	0	
20	axial	0	+	0	0	
21	axial	0	0	-	0	
22	axial	0	0	+	0	
23	axial	0	0	0	-	
24	axial	0	0	0	+	
25	centre	0	0	0	0	
26	centre	0	0	0	0	
27	centre	0	0	0	0	
28	centre	0	0	0	0	

This design allow four main effects to be estimated (A, B, C, D) along with six two-factor interactions (AB, AC, BC, AD, BD, CD), four three-factor interactions (ABC, ABD, ACD, BCD), a four-factor interaction (ABCD) and the sum of squares for A, B, C, D, AB, AC, BC, AD, BD, CD, ABC, ABD, ACD, BCD, and ABCD and eight axial-factor.

Table 3.3.2 and Table 3.3.3 shows the cutting conditions which were chosen and tests were carried out according these set-up cutting conditions. The cutting conditions in Table 3.2b are chosen according to recommendation by SUMITOMO ELECTRIC HARDMETAL that can be refer from Performance Cutting Tools - General Catalogue 07-08. This parameters data are based on the type of cutting tool that be used in this experimental, DNMG110404N-GU Grade AC2000 (TiN coated carbide).

Table 3.3.2: The level of independent variables for the procedures

No	Variable	Symbol	Units	Level		
				Low (-)	Cent.(0)	High (+)
1	Cutting Speed	V	m/min	180	230	280
2	Feed Rate [24]	f	mm/rev	0.07	0.11	0.17
3	Depth of Cut	DOC	mm	0.1	0.15	0.2
4	Tool Overhang	l	mm	22	37	52

Table 3.3.3: The cutting conditions and the groups of experimental testing

NO	RUN		DESIGN FACTOR				CUT LENGTH	Ra
			A	B	C	D		
1	23	(1)	180	0.07	0.1	22	16	
2	2	a	280	0.07	0.1	22	25	
3	21	b	180	0.17	0.1	22	39	
4	16	ab	280	0.17	0.1	22	61	
5	8	c	180	0.07	0.2	22	16	
6	15	ac	280	0.07	0.2	22	25	
7	7	bc	180	0.17	0.2	22	39	
8	6	abc	280	0.17	0.2	22	61	
9	5	d	180	0.07	0.1	52	16	
10	9	ad	280	0.07	0.1	52	25	
11	4	bd	180	0.17	0.1	52	39	
12	3	abd	280	0.17	0.1	52	61	
13	22	cd	180	0.07	0.2	52	16	
14	28	acd	280	0.07	0.2	52	25	
15	19	bcd	180	0.17	0.2	52	39	
16	17	abcd	280	0.17	0.2	52	61	
17	11	axial	180	0.12	0.15	37	32	
18	26	axial	280	0.12	0.15	37	32	
19	14	axial	230	0.07	0.15	37	32	
20	13	axial	230	0.17	0.15	37	32	
21	12	axial	230	0.12	0.1	37	32	
22	18	axial	230	0.12	0.2	37	32	
23	10	axial	230	0.12	0.15	22	32	
24	24	axial	230	0.12	0.15	52	32	
25	20	centre	230	0.12	0.15	37	32	
26	1	centre	230	0.12	0.15	37	32	
27	27	centre	230	0.12	0.15	37	32	
28	25	centre	230	0.12	0.15	37	32	

Note:

1. External cutting length, $L = \text{time machining (t)} \times \text{feed rate (f)} \times \text{revolution per minutes (rpm)}$.
2. Time machining, t has been set to 0.24 minutes (14.4 seconds).
3. $\text{Rpm} = [\text{cutting speed (CS)} \times 1000] / [\pi \times \text{diameter (D)}]$

CHAPTER 4

RESULT AND DISCUSSION

4.1 Strategy of Experiment

Figure 4.1 show a flow chart strategy of experiment. The study has 4 phases to be through before completing the experiment. The 4 phases are discovery phase, breakthrough phase, optimization phase and validation phase. In discovery phase, known and unknown factors need to be identified and screening process need to be done to classified the range of parameter. In this study the factors have been identified and there are cutting speed, feed rate, depth of cut and tool length. The parameters of the factors also have been recognized base on previous study and from manufacturer data.

After completing the first phase (discovery), next phase is breakthrough phase where here we need to estimate effects and interaction by using full factorial as a tool to identify that the model and factors are significant or not significant and interaction between the factors. Besides that we need to identify curvature of the model is significant or not significant to determine the next phase to be continued for further analysis. If the curvature is significant, the data can go for next phase, the optimization phase (higher regression – 2nd orders) and if not significant, the data

jump to last phase, validation phase. It means the data with not significant curvature is remaining with 1st order (linear regression).

A total of sixteen (16) workpieces with added four (4) centre point workpiece were turned in accordance with the experimental design, and each measured for surface roughness three (3) times at approximately 120° intervals around the parts. This helped avoid possibly biased measurements and to insure accuracy of the readings by averaging the natural variations of the surface roughness values. The data than are input into full factorial tool for analysis.

Table 4.1.1: Data for surface finish data by using Full Factorial

No	Run	Design Factors				Cut Length	Surface Finish, Ra			
		A	B	C	D		i	ii	iii	Avg
1	23	180	0.07	0.1	22	16	0.41	0.43	0.45	0.43
2	2	280	0.07	0.1	22	25	0.31	0.31	0.33	0.32
3	21	180	0.17	0.1	22	39	1.20	1.20	1.14	1.18
4	16	280	0.17	0.1	22	61	0.99	1.01	0.97	0.99
5	8	180	0.07	0.2	22	16	0.53	0.54	0.49	0.52
6	15	280	0.07	0.2	22	25	0.33	0.32	0.34	0.33
7	7	180	0.17	0.2	22	39	1.30	1.27	1.21	1.26
8	6	280	0.17	0.2	22	61	0.95	0.95	0.94	0.95
9	5	180	0.07	0.1	52	16	1.10	1.12	1.14	1.12
10	9	280	0.07	0.1	52	25	1.00	0.96	0.95	0.97
11	4	180	0.17	0.1	52	39	1.38	1.37	1.38	1.38
12	3	280	0.17	0.1	52	61	1.11	1.14	1.12	1.12
13	22	180	0.07	0.2	52	16	1.18	1.17	1.17	1.17
14	28	280	0.07	0.2	52	25	0.76	0.75	0.71	0.74
15	19	180	0.17	0.2	52	39	1.60	1.60	1.50	1.60
16	17	280	0.17	0.2	52	61	0.85	0.82	0.76	0.81
17	20	230	0.12	0.15	37	32	0.55	0.63	0.68	0.62
18	1	230	0.12	0.15	37	32	0.84	0.85	0.80	0.83
19	27	230	0.12	0.15	37	32	0.60	0.70	0.65	0.65
20	25	230	0.12	0.15	37	32	0.61	0.51	0.50	0.54

In this experiment the data show that it required higher regression (2nd orders and higher order). Table 4.1.2 show the data is significant in curvature.

Table 4.1.2: ANOVA table show significant curvature that required further analysis

Source	Sum of Squares	df	Mean Square	F Value	p-value Prob > F	
Model	2.23	5	0.45	50.64	< 0.0001	significant
<i>A-CUTTING SP</i>	0.67	1	0.67	76.21	< 0.0001	
<i>B-FEED RATE</i>	0.55	1	0.55	62.06	< 0.0001	
<i>D-TOOL LENG</i>	0.74	1	0.74	83.83	< 0.0001	
<i>AB</i>	0.12	1	0.12	13.88	0.0025	
<i>BD</i>	0.15	1	0.15	17.24	0.0011	
Curvature	0.15	1	0.15	17.16	0.0012	significant
Residual	0.11	13	8.823E-003			
<i>Lack of Fit</i>	0.070	10	6.970E-003	0.46	0.8430	not significant
<i>Pure Error</i>	0.045	3	0.015			
Cor Total	2.50	19				

In optimization phase, we used to estimate the coefficient of the model either the model is linear suggested, 2FI suggested, quadratic suggested or cubic suggested. Next, the optimization condition (in range selected for each factors) can be identify base on the model suggested. In this study, the detail finding of optimization phase is explains in next paragraph 4.2.

Finally, validation phase is used to verify the adequacy of the model developed by comparing between actual data with predicted data and the percentage residual errors are calculated. The detail finding of this study is explained in next paragraph 4.3.

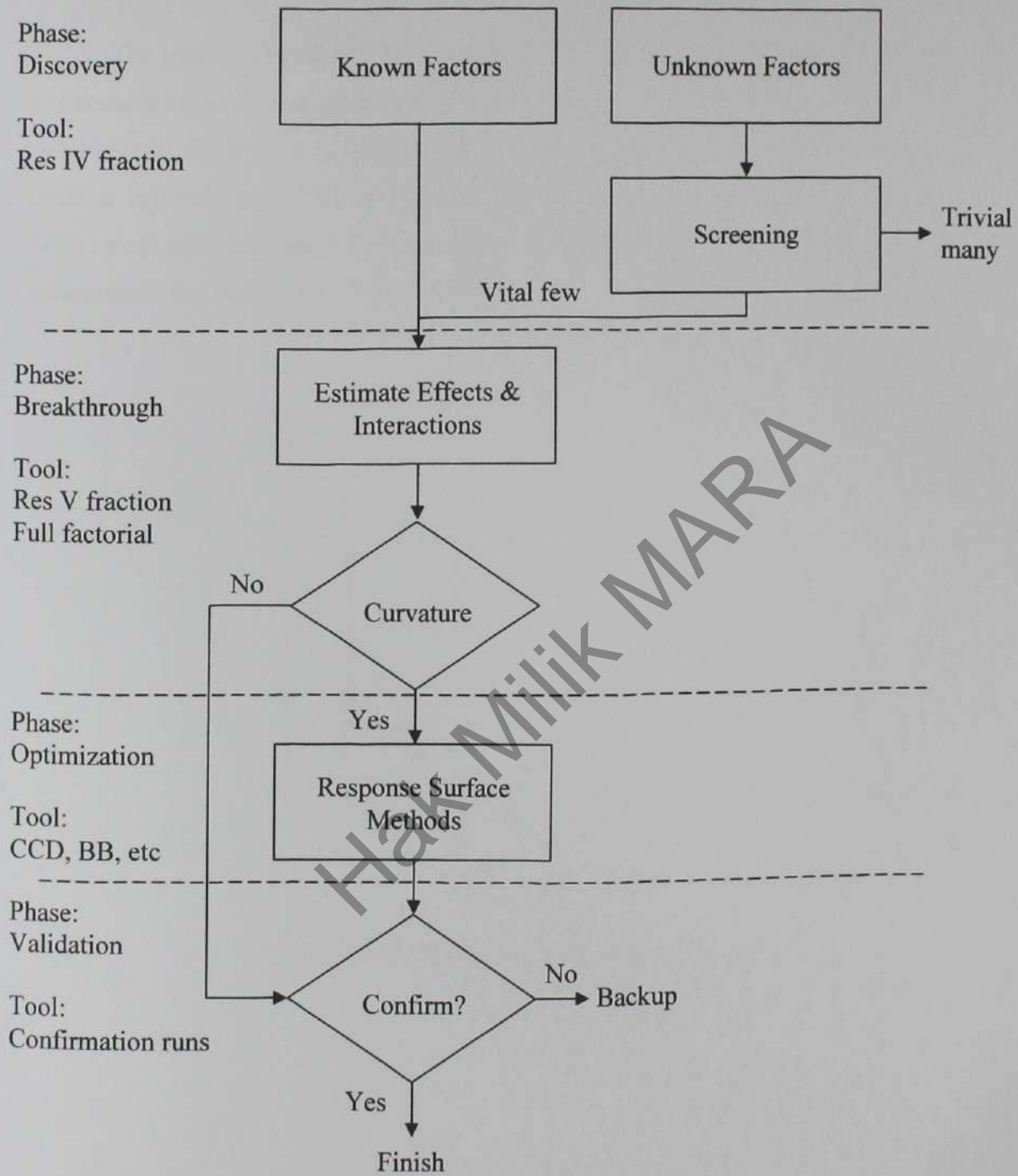


Figure 4.1 Flow Chart Strategy of Experiment

4.2 Central Composite Design (CCD)

The previous twenty (20) workpieces data were used for further analysis with additional another 8 runs (axial point) were taken into CCD analysis to find out for optimization. Each axial point data were measured for surface roughness three (3) times at approximately 120° intervals around the parts. This helped avoid possibly biased measurements and to insure accuracy of the readings by averaging the natural variations of the surface roughness values.

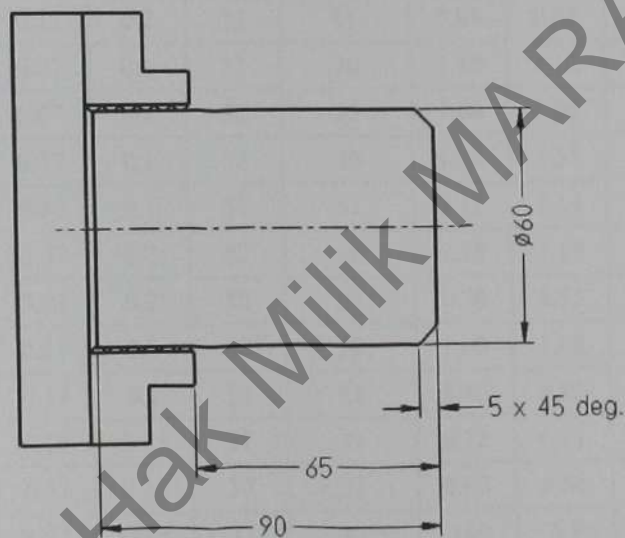


Figure 4.2 Illustration of workpiece dimension

Table 4.2.1: Data for surface finish data by using RSM

No	Run	Design Factors				Cut Length	Surface Finish, Ra			
		A	B	C	D		i	ii	iii	Avg
1	23	180	0.07	0.1	22	16	0.41	0.43	0.45	0.43
2	2	280	0.07	0.1	22	25	0.31	0.31	0.33	0.32
3	21	180	0.17	0.1	22	39	1.20	1.20	1.14	1.18
4	16	280	0.17	0.1	22	61	0.99	1.01	0.97	0.99
5	8	180	0.07	0.2	22	16	0.53	0.54	0.49	0.52
6	15	280	0.07	0.2	22	25	0.33	0.32	0.34	0.33
7	7	180	0.17	0.2	22	39	1.30	1.27	1.21	1.26
8	6	280	0.17	0.2	22	61	0.95	0.95	0.94	0.95
9	5	180	0.07	0.1	52	16	1.10	1.12	1.14	1.12
10	9	280	0.07	0.1	52	25	1.00	0.96	0.95	0.97
11	4	180	0.17	0.1	52	39	1.38	1.37	1.38	1.38
12	3	280	0.17	0.1	52	61	1.11	1.14	1.12	1.12
13	22	180	0.07	0.2	52	16	1.18	1.17	1.17	1.17
14	28	280	0.07	0.2	52	25	0.76	0.75	0.71	0.74
15	19	180	0.17	0.2	52	39	1.60	1.60	1.50	1.60
16	17	280	0.17	0.2	52	61	0.85	0.82	0.76	0.81
17	11	230	0.11	0.15	37	32	0.72	0.71	0.76	0.73
18	26	230	0.11	0.15	37	32	0.63	0.61	0.59	0.61
19	14	230	0.11	0.15	37	32	0.69	0.7	0.7	0.70
20	13	230	0.11	0.15	37	32	0.51	0.54	0.51	0.52
21	12	230	0.12	0.1	37	32	0.56	0.57	0.58	0.57
22	18	230	0.12	0.2	37	32	0.63	0.59	0.58	0.60
23	10	230	0.12	0.15	22	32	0.62	0.62	0.61	0.62
24	24	230	0.12	0.15	52	32	0.75	0.77	0.90	0.81
25	20	230	0.12	0.15	37	32	0.55	0.63	0.68	0.62
26	1	230	0.12	0.15	37	32	0.84	0.85	0.80	0.83
27	27	230	0.12	0.15	37	32	0.60	0.70	0.65	0.65
28	25	230	0.12	0.15	37	32	0.61	0.51	0.50	0.54

The results from the machining trials performed as the experimental plan are shown in Table 4.2.1. These results were input into the Design Expert Software for further analysis. Response surface methodology (RSM) design called Central

Composite Design CCD was used to estimate the coefficient of a quadratic model. By perform natural log on transformation box (recommended transform to natural log by diagnostics tool (box cox)), examination of Fit Summary shows the resulting (computer generated) for quadratic model that is statistically significant for surface roughness response and therefore it will be used for further analysis. Table 4.2.2 shows summary program calculates the effects for all model terms (F-values, lack of fit and R-squared values).

Table 4.2.2: If a statistically significant model is detected, the program will underline and note the "Suggested" model. The table show quadratic model is suggested.

Response	1	rA	Transform:	Natural Log	Constant:
*** WARNING: The Cubic Model and higher are Aliased! ***					
Summary (detailed tables shown below)					
Source	Sequential p-value	Lack of Fit p-value	Adjusted R-Squared	Predicted R-Squared	
Linear	< 0.0001	0.3298	0.6736	0.5576	
2FI	0.0309	0.5062	0.7889	0.6206	
<u>Quadratic</u>	<u>0.0332</u>	<u>0.7494</u>	<u>0.8701</u>	<u>0.7676</u>	<u>Suggested</u>
Cubic	0.5663	0.7156	0.8630	0.2499	Aliased

In order to analyze a factorial design, the significant factor effects must be identified and separated from the insignificant effects. Clicking on the Effects button starts the regression calculations to compute a table of effects for model terms. By selecting the backward elimination (alpha out 0.05) procedure to automatically reduce the terms that are not significant, the resulting ANOVA table for the reduced quadratic model for surface roughness is shown in Table 4.2.3. An ANOVA table commonly used to summarize the test performed; test for significance of the regression model, test for significance on individual model coefficient and test for lack-of fit.

Table 4.2.3: ANOVA table for response surface quadratic model

ANOVA for Response Surface Reduced Quadratic Model						
Analysis of variance table [Partial sum of squares - Type III]						
Source	Sum of Squares	df	Mean Square	F Value	p-value Prob > F	
Model	4.31	5	0.86	43.36	< 0.0001	significant
A-CUTTING SP	0.91	1	0.91	45.70	< 0.0001	
B-FEED RATE	1.04	1	1.04	52.28	< 0.0001	
D-TOOL LENG	1.48	1	1.48	74.34	< 0.0001	
BD	0.59	1	0.59	29.49	< 0.0001	
D ²	0.30	1	0.30	14.98	0.0008	
Residual	0.44	22	0.020			
Lack of Fit	0.34	19	0.018	0.56	0.8166	not significant
Pure Error	0.096	3	0.032			
Cor Total	4.75	27				

The value of "Prob > F" in Table 4.2.3 for model is less than 0.05 which indicates that the model is significant, which is desirable as it indicates that the term in the model have a significant effect on the response. In the same manner, the main effects of cutting speed (A), feed rate (B), tool length (D), the two level of interaction BD and D² are significant model terms. Others model terms are not significant. This insignificant model terms not counting those required for supporting the hierarchy.

The "Lack of Fit F-value" of 0.56 implies the Lack of Fit is not significant relative to the pure error. There is a 81.66% chance that a "Lack of Fit F-value" this large could occur due to noise. Non-significant lack of fit is good. This is desirable as we want the model to fit.

Table 4.2.4 shows that the R-squared value is high close to 1, which is desirable. The "Pred R-Squared" of 0.8589 is in reasonable agreement with the "Adj R-Squared" of 0.8869. A rule of thumb is that the adjusted and predicted R-

squared values should be within 0.2 of each other. "Adeq Precision" measures the signal to noise ratio. A ratio greater than 4 is desirable and ratio of 23.028 indicates an adequate signal. This model can be used to navigate the design space.

Table 4.2.4: ANOVA table for R-square

Std. Dev.	0.14	R-Squared	0.9079
Mean	-0.33	Adj R-Squared	0.8869
C.V. %	42.20	Pred R-Square	0.8589
PRESS	0.67	Adeq Precisor	23.028

The following equation is the final empirical models in terms of coded factors for surface roughness:

$$\ln(rA) = -0.47 - 0.22 \times A + 0.24 \times B + 0.29 \times D - 0.19 \times BD + 0.22 \times D^2$$

While, the following equation is the final empirical models in term of actual factors for surface roughness:

$$\ln(rA) = -0.54606 - 4.49342E-003 \times \text{CUTTING SPEED} + 14.24890 \times \text{FEED RATE} - 0.021063 \times \text{TOOL LENGTH} - 0.25522 \times \text{FEED RATE} \times \text{TOOL LENGTH} + 9.56666E-004 \times \text{TOOL LENGTH}^2$$

Graphical summaries for case statistics can be seen by selecting the Diagnostics button. Most of the plots display residuals, which show how well the model satisfies the assumptions of the analysis of variance. The normal probability plots of the residuals and the plots of the residuals versus the predicted response for surface roughness are shown in Figure 4.1.1 and 4.1.2.

The normal probability plot indicates whether the residuals follow a normal distribution, in which case the points will follow a straight line. A check on the plots in Figure 4.2.2 revealed that the residual generally fall on the straight line implying that the errors are distributed normally. This implies that the model proposed is adequate assumptions.

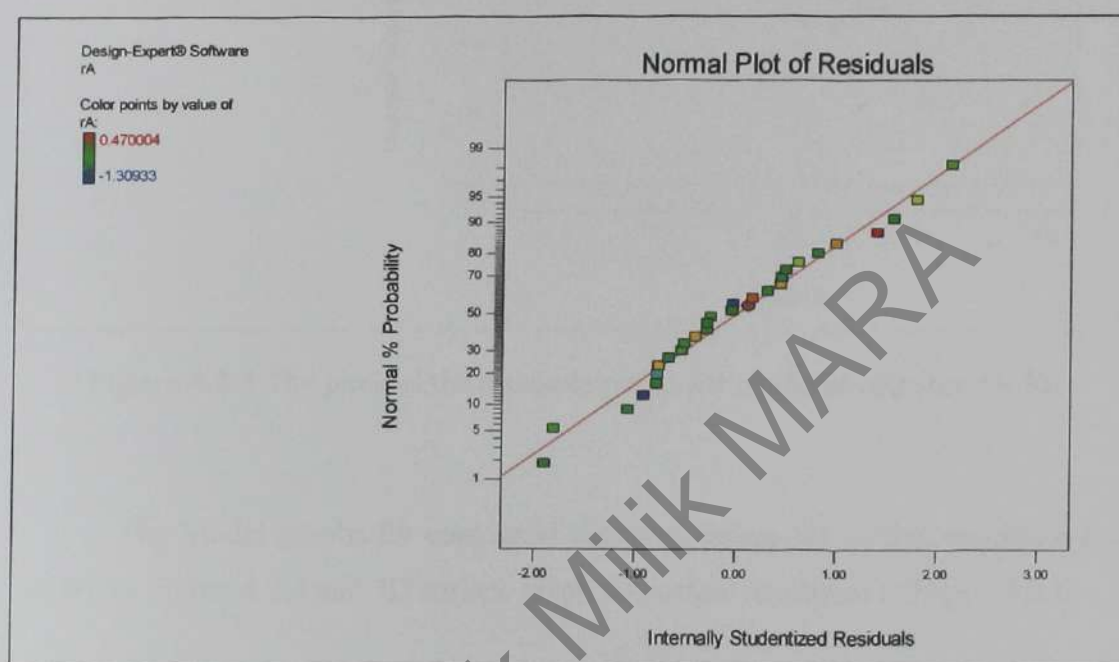


Figure 4.2.2 The normal probability plots of residuals for surface roughness

Also Figure 4.2.3 is a plot of the residuals versus the ascending predicted response values. It tests the assumption of constant variance. The plot should be a random scatter (constant range of residuals across the graph.) and the figure revealed that they have no obvious pattern and unusual structure. This implies that the models proposed are adequate and there are no reasons to suspect any violation of the independence or constant variance assumption.

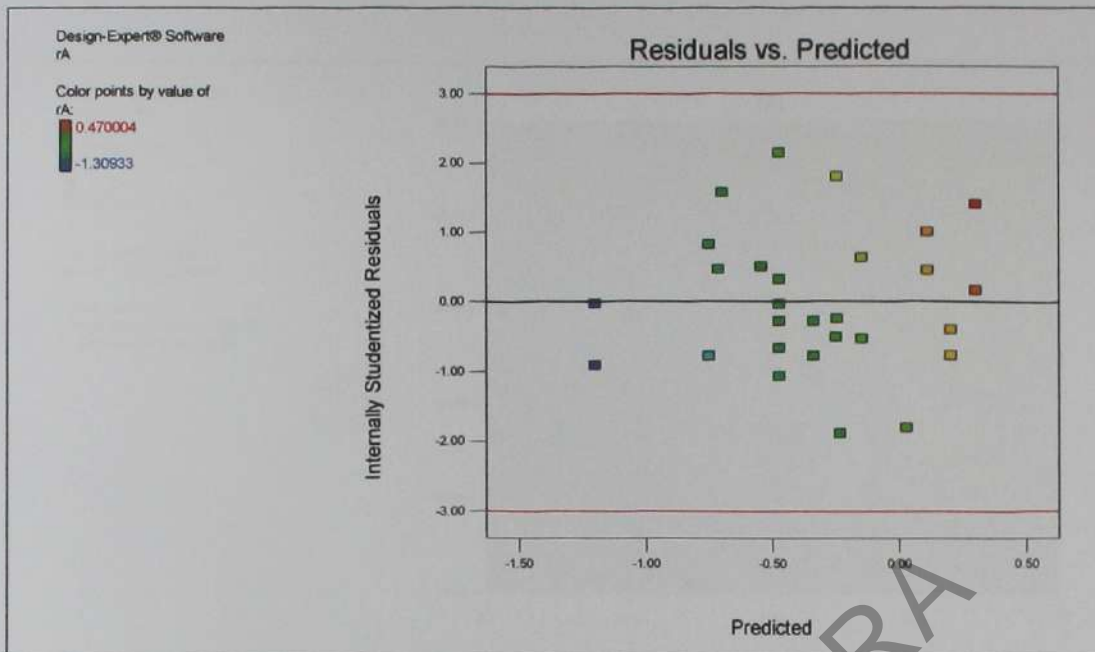


Figure 4.2.3 The plots of the residuals versus the predicted response for Ra

The Model graphs for contour of response surface for surface roughness are shown in Figure 4.2.4 and 3D surface graph for surface roughness in Figure 4.2.5.

The graphs have curvilinear profile in accordance to the quadratic model fitted. It is clear from Figure 4.1c and 4.1d that at any particular of depth of cut, the best surface finish is obtainable when the tool length and feed rate at the lowest range and cutting speed at the highest range of experimented (blue region). This is consistent with the fact that the cutting speed (A), feed rate (B), tool length (D) and tool length² (D²) terms are significant. Depth of cut is not significant in this experimented.

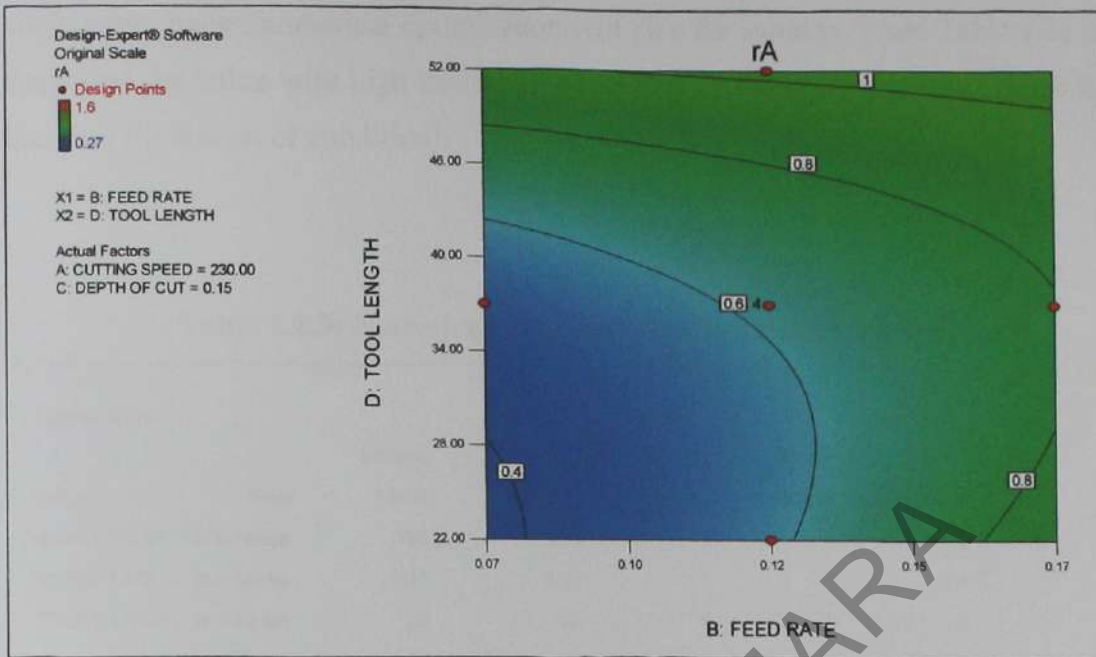


Figure 4.2.4 Ra contours in B-D plane at CS of 230 m/min and DOC 0.15 mm

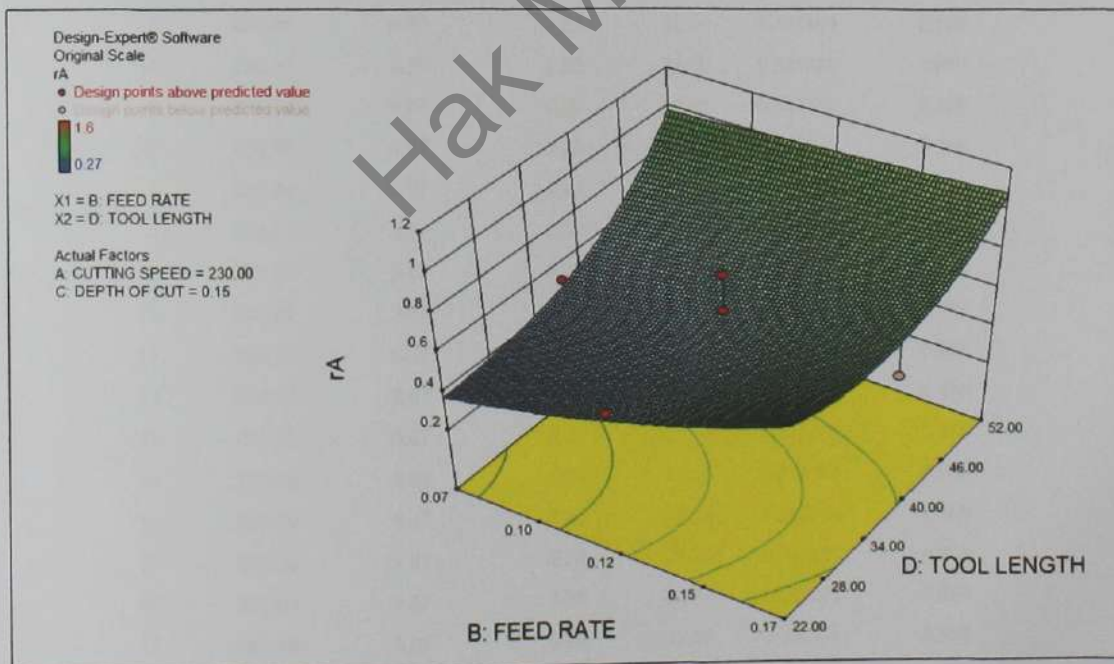


Figure 4.2.5 3D surface model in feed-tool length plane at CS of 230 m/min and DOC 0.15 mm

In order to find a good set of condition (maximum value for the range) for surface roughness, numerical optimization will give the solution. From Table 4.2e is suggested the value with high desirability is recommendation for optimum value in this case (in this set of condition).

Table 4.2.5: Numerical optimization table found 21 solution

Constraints						
Name	Goal	Lower Limit	Upper Limit	Lower Weight	Upper Weight	Importance
A:CUTTING SP	is in range	180	280	1	1	3
B:FEED RATE	is in range	0.07	0.17	1	1	3
D:TOOL LENG	is in range	22	52	1	1	3
rA	minimize	0.27	1.6	1	1	3

Solutions						
Number	CUTTING SPEI	FEED RATE	DEPTH OF CUT*	TOOL LENGTH	rA	Desirability
1	280.00	0.07	0.20	22.00	0.301133	0.977
2	280.00	0.07	0.20	22.12	0.301257	0.976
3	280.00	0.07	0.20	22.34	0.301486	0.976
4	280.00	0.07	0.20	22.60	0.301808	0.976
5	279.50	0.07	0.20	22.01	0.301814	0.976
6	280.00	0.07	0.20	22.00	0.302297	0.976
7	280.00	0.07	0.20	23.00	0.302379	0.976
8	278.74	0.07	0.20	22.00	0.302846	0.975
9	278.14	0.07	0.20	22.00	0.303662	0.975
10	280.00	0.07	0.20	23.77	0.303732	0.975
11	276.72	0.07	0.20	22.00	0.305607	0.973
12	278.04	0.07	0.20	25.28	0.310134	0.970
13	273.28	0.07	0.20	22.00	0.310368	0.970
14	273.10	0.07	0.20	22.64	0.311368	0.969
15	280.00	0.07	0.20	22.19	0.312734	0.968
16	280.00	0.07	0.20	27.91	0.317264	0.964
17	267.89	0.07	0.20	24.63	0.32275	0.960
18	260.46	0.07	0.20	22.00	0.328774	0.956

Figure 4.2.6 shows optimization in term of contour and Figure 4.2.7 show optimization in term of 3D model surface. The red color is the high desirability value that is recommended for good set of condition.

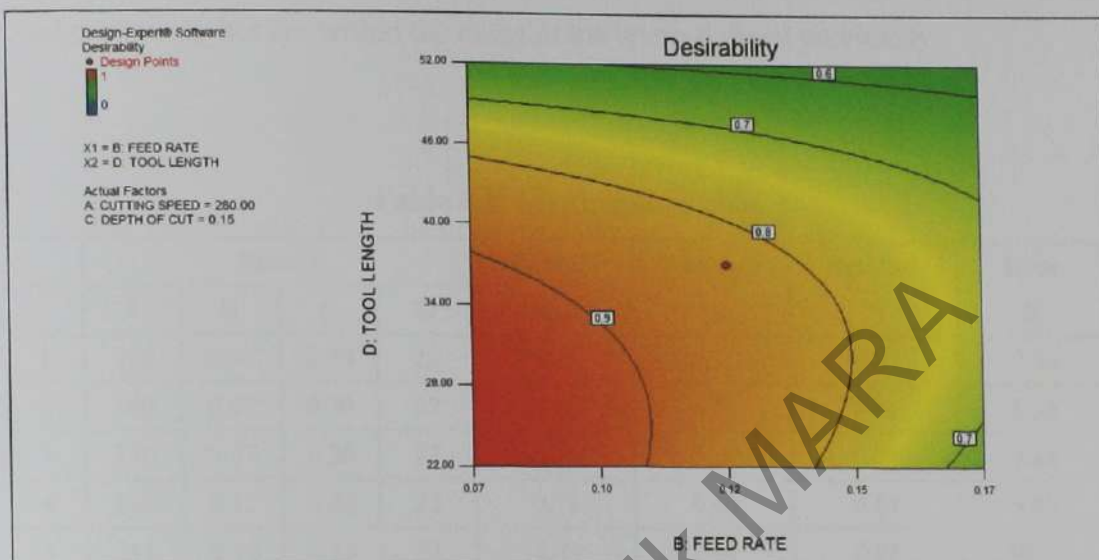


Figure 4.2.6 Desirability contours in feed-tool length plane at cutting speed of 280 m/min and depth of cut 0.15 mm

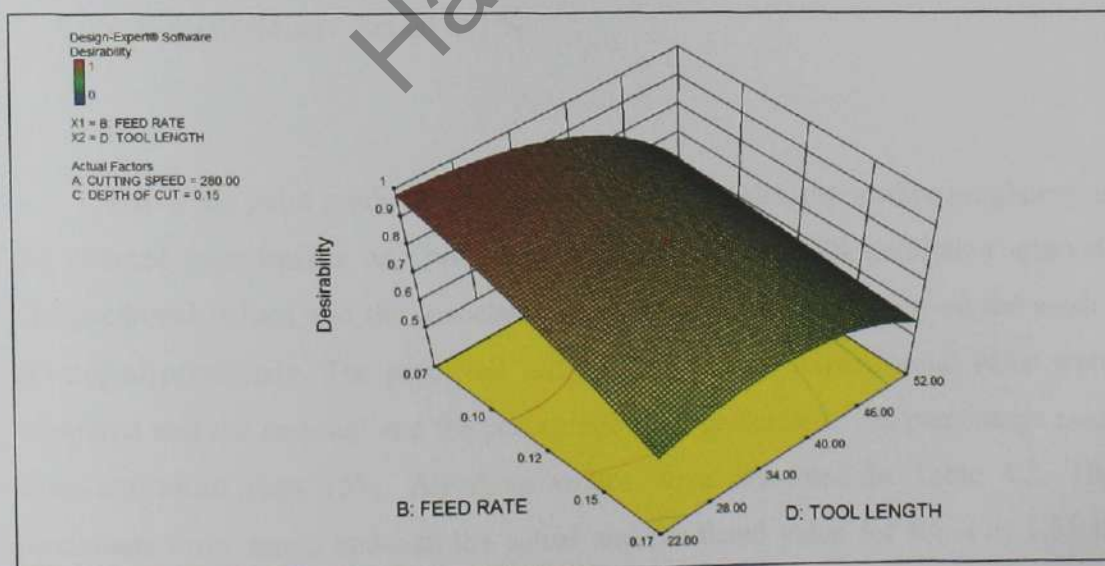


Figure 4.2.7 3D surface model in feed-tool length plane at cutting speed of 230 m/min and depth of cut 0.15 mm

4.3 Confirmation Test

In order to verify the adequacy of the model developed, six confirmation run experiments were performed as shown in Table 4.3. The test condition for six confirmation run experiments were among the cutting conditions that have not been used previously but are within the range of the levels defined previously.

Table 4.3: Confirmation table

No	Factors				Actual Ra	Predicted Ra	Residual	Error %
	A	B	C	D				
1	270	0.07	0.20	22	0.30	0.31	-0.01	-3.33
2	260	0.07	0.20	22	0.36	0.33	0.03	8.33
3	250	0.07	0.20	22	0.35	0.34	0.01	2.86
4	260	0.15	0.20	22	0.73	0.66	0.07	9.59
5	255	0.10	0.15	22	0.49	0.44	0.05	10.20
6	200	0.13	0.20	52	1.21	1.19	0.02	1.65

Note:

1. Residual = Actual r_A - Predicted r_A
2. Error % = (Residual / Actual r_A) %

Using the point prediction capability of the software, the surface roughness of the selected experiments was predicted together with the 95% prediction interval. The predicted values and the associated prediction interval are based on the model developed previously. The predicted value and the actual experimental value were compared and the residual and the percentage error calculated. The percentage error must not more than 15%. All these values were presented in Table 4.3. The percentage error range between the actual and predicted value for R_a is as 1.65 to 10.20%. It can be said that the empirical models developed were reasonably accurate. All the actual values for the confirmation run are within the 95% prediction interval. The 95% prediction interval is the range in which we can expect any individual value to fall into 95% of the time.

4.4 Discussion

Notice that the main effects of cutting speed A, feed rate B and tool length D together with two level interaction of feed rate – tool length BD and second order effect tool length D^2 are the significance model term. The main effect of D is most significant factor associated with surface roughness followed by effects of B, A, BD and D^2 .

4.4.1 Interaction between Tool Overhang, D and Feed Rate, B

Tool overhang and feed rate are interact and influence each other in producing an effective result on surface roughness. Figure 4.3.1 show the interaction between tool length and feed rate at cutting speed 230 mm/min and depth of cut 0.15 mm. The black color represent a short tool overhang, 22 mm and red color represent a long tool overhang, 52 mm. The figure show that when feed rate at low condition, 0.07 mm/rev it produce a good surface roughness and when the feed rate at high range, 0.17 mm/rev the surface roughness value is increasing and producing a poor surface roughness. The figure also revealed that, long tool overhang increasing in surface roughness value (poor surface roughness) when compared to short tool overhang (better surface roughness). The surface roughness of work piece is proportional to cutting tool overhang and feed rate. The surface roughness is better when the feed rate is lower, 0.07 mm/rev and the tool overhang is short, 22 mm

Cutting tool vibration has a significant effect on surface roughness of workpiece. Long tool overhang will produced a high vibration and produces a poor surface finish than the short tool overhang. The vibration of cutting tool depends strongly on cutting tool overhang [25].

Feed rate is among major factor that has a direct impact on surface roughness [26]. The workpiece machined with a smaller feed rate, the machined surface shows that extensive material side plastic flow existed [27]. This explains the better surface finish obtained at lower feed rates. A lower feed rate increased the area in which the chip thickness was lower than the minimum chip thickness. Hence, instead of cutting, a large part of the material was ploughed, which led to material side flow.

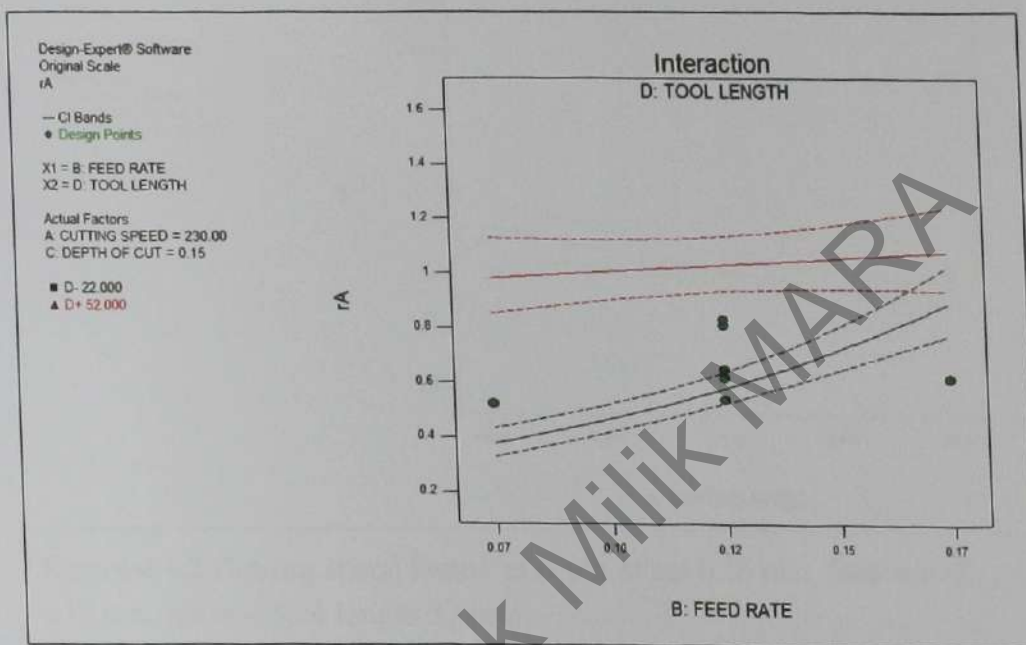


Figure 4.4.1 Interaction Feed-Tool Length factor at cutting speed 230 mm/min and DOC 0.15 mm. D- (22mm) D+ (52mm).

4.4.2 Cutting Speed

Cutting speed another major impacts on surface roughness. Cutting speed at lower range produces a high value surface roughness. It means a poor surface roughness. It affects the surface roughness when operating at lower speed, which leads to the formation of a built-up edge.

Cutting speed at higher range produces a low value surface roughness and good surface roughness. Higher speeds are important in yielding accurate results. At speeds higher actual surface roughness comes closer to the calculated value of surface roughness [28]. Cutting speed does not interact and influence by other factors in this experiment.

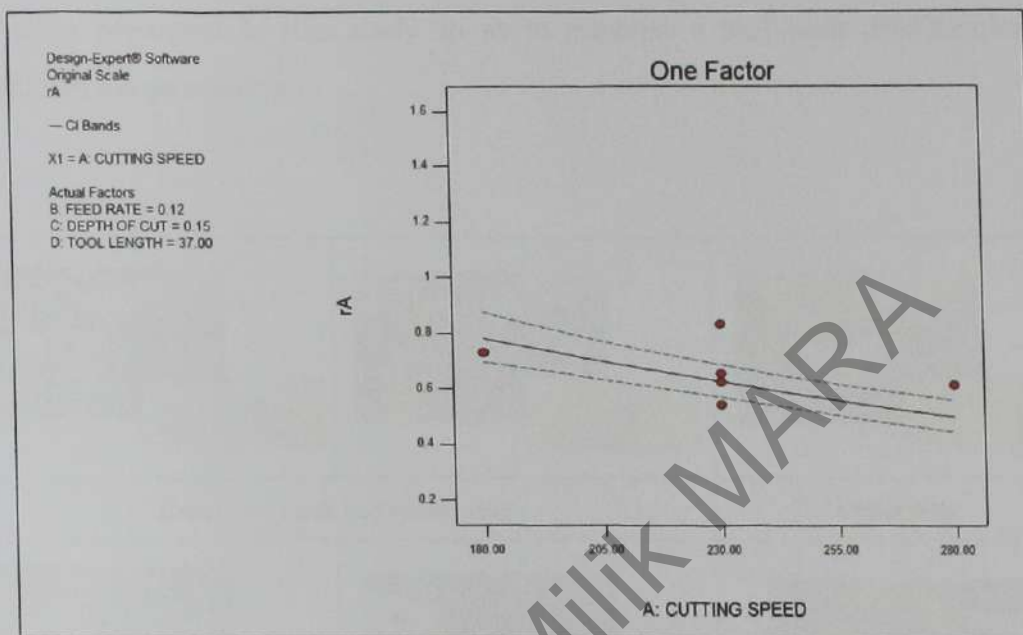


Figure 4.4.2 Cutting speed factor at depth of cut 0.15 mm, feed rate of 0.12 mm/rev and tool length 37 mm.

4.4.3 Depth of Cut

The depth of cut has a proven effect on tool life and cutting forces but it has no significant effect on surface roughness for this experiment (finishing condition). Therefore, a larger depth of cut can be used to save machining time when machining small quantities of workpieces. On the other hand, combining a low depth of cut with a higher cutting speed prevents the formation of a built-up edge, thereby aiding the process by yielding a better surface finish [29].

4.5. Tool Wear








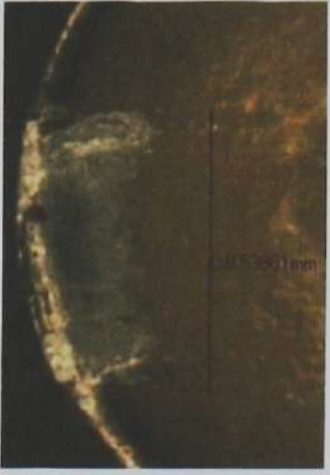

Figure 4.5 show the tool wear types according to Metalcutting Technical Guide Sandvick 2008. Tool wear obtained from the tests carried out on the Aluminum alloys 6061 has been classified according to the tool failure types shown in that standard. The objective of this study is to identify the type of tool wear in all the cases presented in this study so as to establish a tool wear classification of aluminum alloys material.



Figure 4.5 Tool wear classification according to Metalcutting Technical Guide [14]

4.5.1. Table of Tool Wear Data for Actual Experiment

Table 4.5.1.1: Table of tool wear for actual data (100x magnificant)

		
1. A 180, B 0.07, C 0.1, D 22, Ra 0.43, Crater wear	2. A 280, B 0.07, C 0.1, D 22, Ra 0.32, Crater wear	3. A 180, B 0.17, C 0.1, D 22, Ra 1.18, Crater wear
		
4. A 280, B 0.17, C 0.1, D 22, Ra 0.99, Crater wear	5. A 180, B 0.07, C 0.2, D 22, Ra 0.52, Crater wear	6. A 280, B 0.07, C 0.2, D 22, Ra 0.33, Crater wear
		
7. A 180, B 0.17, C 0.2, D 22, Ra 1.26, Crater wear	8. A 280, B 0.17, C 0.2, D 22, Ra 0.95, Crater wear	9. A 180, B 0.07, C 0.1, D 52, Ra 1.12, Crater wear

		
10. A 280, B 0.07, C 0.1, D 52, Ra 0.97, Crater wear	11. A 180, B 0.17, C 0.1, D 52, Ra 1.38, Crater wear	12. A 280, B 0.17, C 0.1, D 52, Ra 1.12, Crater wear
		
13. A 180, B 0.07, C 0.2, D 52, Ra 1.17, Crater wear	14. A 280, B 0.07, C 0.2, D 52, Ra 0.74, Crater wear	15. A 180, B 0.17, C 0.2, D 52, Ra 1.60, Crater wear
		
16. A 280, B 0.17, C 0.2, D 52, Ra 0.81, Crater wear	17. A 230, B 0.11, C 0.15, D 37, Ra 0.73, Crater wear	18. A 230, B 0.11, C 0.15, D 37, Ra 0.61, Crater wear

		
19. A 230, B 0.11, C 0.15, D 37, Ra 0.70, Crater wear	20. A 230, B 0.11, C 0.15, D 37, Ra 0.52, Crater wear	21. A 230, B 0.12, C 0.1, D 37, Ra 0.57, Crater wear
		
22. A 230, B 0.12, C 0.2, D 37, Ra 0.60, Crater wear	23. A 230, B 0.12, C 0.15, D 22, Ra 0.62, Crater wear	24. A 230, B 0.12, C 0.15, D 52, Ra 0.81, Crater wear
		
25. A 230, B 0.12, C 0.15, D 37, Ra 0.62, Crater wear	26. A 230, B 0.12, C 0.15, D 37, Ra 0.83, Crater wear	27. A 230, B 0.12, C 0.15, D 37, Ra 0.65, Crater wear



28. A 230, B 0.12, C 0.15, D 37,

Ra 0.54, Crater wear

Hak Milik MARA

4.5.2 Discussion

Examination of the worn insert for all condition revealed that the coating was rapidly removed from the substrate. All worn insert has a similar pattern of wear (wear on rake face) except the length of affected area is different. By comparing to the tool type chart Figure 4.5, show that the examination of the worn inserts similar to the crater wear type. The observation shows that the length of affected area is getting larger according to increasing the depth of cut in parameter. It seems the worn insert in this study only affected by depth of cut not from other factors (cutting speed, feed rate and tool overhang).

The worn inserts have the same pattern is because due to finishing cut type, where the range of depth of cut is not obviously different (0.07 – 0.17). In addition the time machining is short (0.24 minutes) and the cutting distance also short (16 – 61 mm).

Crater wear involves a gradual loss of material that progresses on the rake face of the tool during cutting. The abrasive wear takes place in the region of sliding contact between the chip and the face and usually occurs when continuous chip is produced. Severe rake face wear usually result from the temperature activated diffusion wear mechanism. Excessive crater wear weakens the cutting edge and can lead to deformation or fracture of the tool.

Table 4.5.1.2: Comparison of tool wear (crater wear on rake face)



* A: Cutting Speed, m/min

B: Feed Rate, mm/rev

C: Depth of Cut, mm

D: Tool Overhang, mm

4.6 Chip Formation

Figure 4.6 reproduces the chip types recognized in the standard ISO 3685 [30]. Chips obtained from the tests carried out on the Aluminum alloys 6061 has been classified according to the chip types shown in that standard. It is important remark that this standard was developed for turning steel and cast iron workpieces and, therefore, at this first analysis, only the shape of the chips has been taken into account but not the classification in the two big categories, favorable and unfavorable, given by ISO. The reason is it has been detected that such classification, good for the steels and cast irons, cannot be adequate for the aluminum and its alloys [31].

Because of this, it will be necessary to analyze all the cases presented in this study so as to establish a chips classification of aluminum and aluminums alloys material similar to the existent ISO 3685 for the steels.




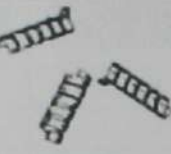




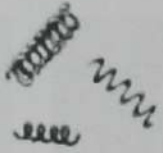
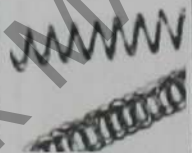
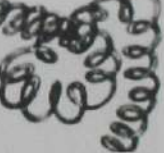

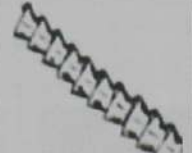





CUTTING		FAVOURABLE		UNFAVOURABLE	
STRAIGHT	1. RIBBON CHIPS	1.2. SHORT		1.1. LONG	1.3. SNARLED
					
MAINLY UP CURLING	2. TUBULAR CHIPS	2.2. SHORT		2.1. LONG	2.3. SNARLED
					
	3. SPIRAL CHIPS			3.1. FLAT	3.2. CONICAL
					
MAINLY SIDE CURLING	4. WASHER TYPE CHIPS	4.2. SHORT		4.1. LONG	4.3. SNARLED
					
UP AND SIDE CURLING	5. CONICAL HELICAL CHIPS	5.2. SHORT		5.1. LONG	5.3. SNARLED
					
	6. ARC CHIPS	6.1. CONNECT.	6.2. LOOSE		
					
	7-8. NATURAL BROKEN CHIPS	7.0. ELEMENTAL			8.0. NEEDLE
					

Figure 4.6 Chip form classification. Adapted from ISO 3685:1993 [29]

4.6.1 Table of Chip Formation Data for Actual Experiment

Table 4.6.1.1: Table of chip formation data for actual experiment (80xmagnificent)

		
1. A 180, B 0.07, C 0.1, D 22, Ra 0.43, 4.3 - Snarled	2. A 280, B 0.07, C 0.1, D 22, Ra 0.32, 4.3 - Snarled	3. A 180, B 0.17, C 0.1, D 22, Ra 1.18, 1.3 - Snarled
		
4. A 280, B 0.17, C 0.1, D 22, Ra 0.99, 2.3 - Snarled	5. A 180, B 0.07, C 0.2, D 22, Ra 0.52, 2.3 - Snarled	6. A 280, B 0.07, C 0.2, D 22, Ra 0.33, 2.3 - Snarled
		
7. A 180, B 0.17, C 0.2, D 22, Ra 1.26, 1.3 - Snarled	8. A 280, B 0.17, C 0.2, D 22, Ra 0.95, 1.3 - Snarled	9. A 180, B 0.07, C 0.1, D 52, Ra 1.12, 2.3 - Snarled
		
10. A 280, B 0.07, C 0.1, D 52, Ra 0.97, 2.3 - Snarled	11. A 180, B 0.17, C 0.1, D 52, Ra 1.38, 1.3 - Snarled	12. A 280, B 0.17, C 0.1, D 52, Ra 1.12, 1.3 - Snarled
		
13. A 180, B 0.07, C 0.2, D 52, Ra 1.17, 2.3 - Snarled	14. A 280, B 0.07, C 0.2, D 52, Ra 0.74, 1.3 - Snarled	15. A 180, B 0.17, C 0.2, D 52, Ra 1.60, 1.3 - Snarled

		
16. A 280, B 0.17, C 0.2, D 52, Ra 0.81, 2.3 - Snarled	17. A 230, B 0.11, C 0.15, D 37, Ra 0.73, 1.3 - Snarled	18. A 230, B 0.11, C 0.15, D 37, Ra 0.61, 2.3 - Snarled
		
19. A 230, B 0.11, C 0.15, D 37, Ra 0.70, 1.3 - Snarled	20. A 230, B 0.11, C 0.15, D 37, Ra 0.52, 1.3 - Snarled	21. A 230, B 0.12, C 0.1, D 37, Ra 0.57, 2.3 - Snarled
		
22. A 230, B 0.11, C 0.2, D 37, Ra 0.60, 2.3 - Snarled	23. A 230, B 0.12, C 0.15, D 22, Ra 0.62, 1.3 - Snarled	24. A 230, B 0.12, C 0.15, D 52, Ra 0.81, 1.3 - Snarled
		
25. A 230, B 0.12, C 0.15, D 37, Ra 0.62, 1.3 - Snarled	26. A 230, B 0.12, C 0.15, D 37, Ra 0.83, 1.3 - Snarled	27. A 230, B 0.12, C 0.15, D 37, Ra 0.65, 1.3 - Snarled
		
28. A 230, B 0.12, C 0.15, D 37, Ra 0.54, 1.3 - Snarled		

4.6.2 Discussion

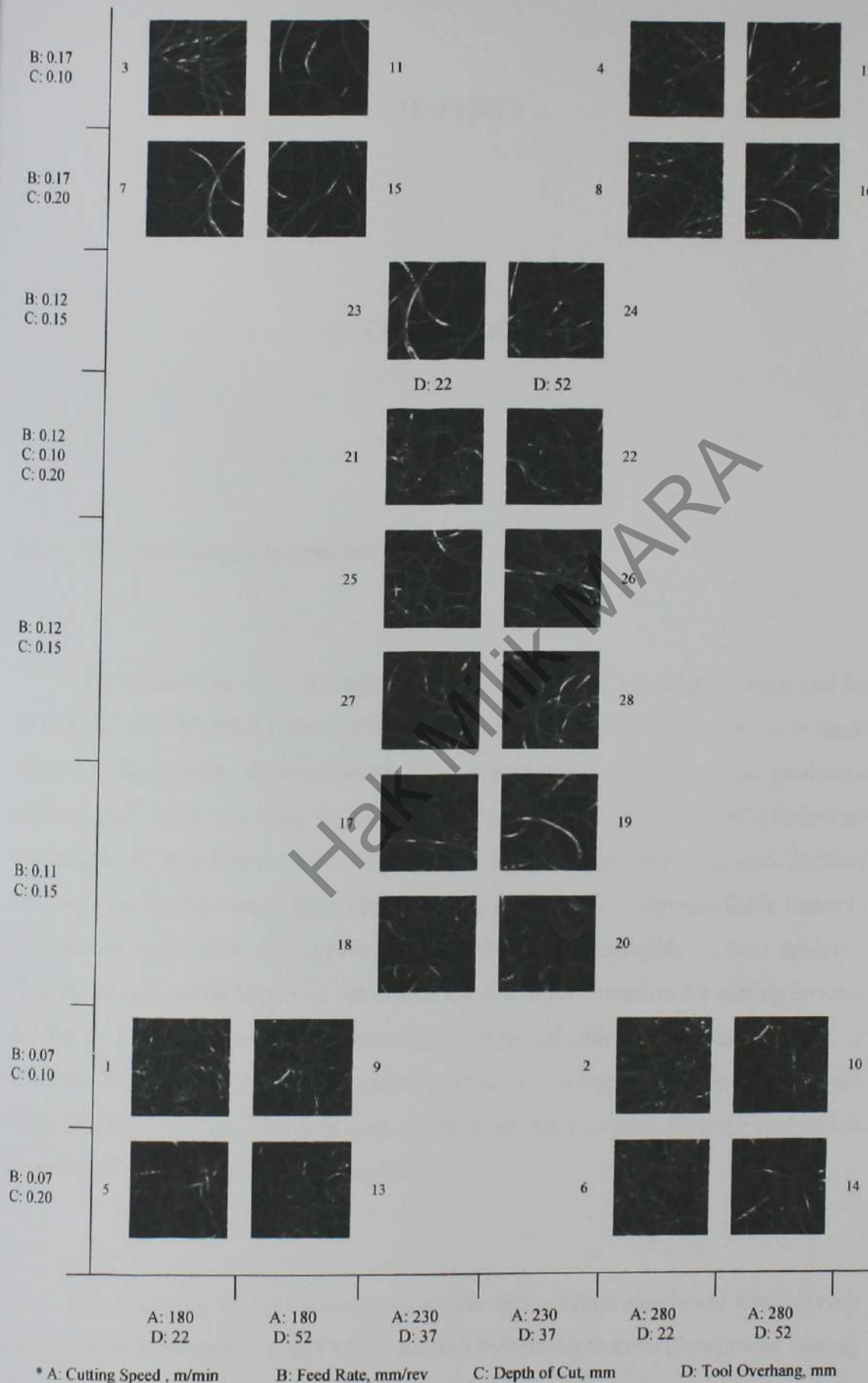
Table 4.6.1a represents the data of chip formation for actual data. It shows that by comparing the data with Figure 4.6, snarled shapes are dominated the pattern of chip formations. There are three (3) types of snarled - 1.3. Snarled (ribbon chip), 2.3. Snarled (tubular chip), and 4.3. Snarled (washer type chip). The relation found between chip formation and feed rate that when increase in feed rate the chip formation getting straight snarled and if decrease in feed rate become curly and curlier snarled chip formation.

The continuous chip is characterized by a general flow of the separated metal along the tool face. There may be some cracking of the chip but in this case it usually does not extend far enough to cause fracture. This chip formed at the higher cutting speed when machining ductile materials. There is little tendency for the material to adhere to the tool. The continuous chips usually show a good cutting ratio and tend to produce the optimum surface finish, but it may become an operating hazard.

The continuous chip characteristics:

- i. cut ductile material
- ii. small uncut thickness
- iii. high cutting speed, and
- iv. large rake angle.

Table 4.6.1.2: Comparison of chip formation



CHAPTER 5

CONCLUSION

5.1 Why tool length is been investigate?

The reason choose tool length as a study is because a standard cutting tool for 20 x 20 mm SUMITOMO came with length 129 mm (from end of tool body to insert tip) and because of the different turret for different brand of machine will produce a different tool length overhang for example DMG CTX 310 GILDIMEISTER the tool overhang is 52 mm and for OKUMA LCS-15 the tool overhang is 22 mm. Besides that many previous journals have identified that tool length is uncontrollable factor in their studies where this uncontrollable factor has been negligible in their analysis. Thru this investigation hope can determine the optimum condition for cutting process and the data can be compiled to develop a series of charts which can be used to eliminate an element of setup waste related to turning operations within the manufacturing industry. The data also can be a reference to manufacturer tool maker to produce a suitable cutting tool length.

This study is to find a correlation between surface roughness and varying cutting tool in turning by using DOE method. Dry cutting tests (without using cutting fluid) are conducted to simulate a good turning, the dry turning provided a clean

environment to obtain undisturbed clear cutting vibration, which results in more accurate and clear correlation between cutting vibrations and roughness. Examine the relationship that exists between the length, at a specific diameter, and surface roughness of bar stock in unsupported turning operations in an attempt to reduce setup waste in turning operations. This paper has a detailed description of the effect of cutting tool overhang on surface roughness of workpiece. The surface roughness of machined parts is predicted by using the surface roughness (R_a) data. The discussion of the results in this investigation can be concluded with the following points. Cutting tool overhang has a significant effect on surface roughness of workpiece. The surface roughness of work piece is proportional to cutting tool overhang. This effect interacts with other independent variables such as feed rate and cutting speed.

1. The vibration of the cutting tool increases with the increasing of the cutting tool overhang for different cutting conditions. Thus the vibration of cutting tool depends strongly on cutting tool overhang.
2. With the increasing feed rate the surface roughness of work piece will increase. The feed rate can be considered as a main cutting factor in the machining operation.
3. Increasing cutting speed leads to a decrease in surface roughness of workpiece.
4. Depth of cut has small effect on surface roughness of work piece in this study.

The observation shows that the worn insert has a similar pattern for all condition parameter, crater wear. The length of affected area on cutting tool is getting larger according to increasing the depth of cut in parameter. It seems the worn insert in this study only affected by depth of cut not from other factors (cutting speed, feed rate and tool overhang). Examination of the chip formation for all condition revealed that snarled shapes are dominated the pattern of chip formations. The observation shows the relationship between chip formation and feed rate that when increase in feed rate the chip formation getting straight snarled and if decrease in feed rate becomes curly and curlier snarled chip formation.

5.2 Recommendations

This study has addressed an area that has been neglected in the past. Now that the initial research has now been conducted for this specific topic, surface roughness of unsupported workpiece in dry cutting, a methodology is available to those who wish to continue with this effort. Future work should include studies that explore the following:

1. Different workpiece diameters
2. Different workpiece materials
3. Dry cutting versus with coolant
4. Different coolant type
5. Supported versus unsupported workpiece
6. Larger sample sizes

Using the same workpiece material, the chart can be broadened to include a wide range of diameters and lengths applicable to this particular material. An example of one possible configuration is the future unsupported workpiece in dry cutting reference chart, illustrated in Table 5. Comprehensive data can be compiled to develop a series of charts which can be used to eliminate an element of setup waste related to turning operations within the manufacturing industry.

Table 5.2: Future Unsupported Workpiece in Dry Cutting Reference Table

	W/piece Length 60		W/piece Length 65		W/piece Length 70	
	supported	unsupported	supported	unsupported	supported	unsupported
Dry						
Coolant						

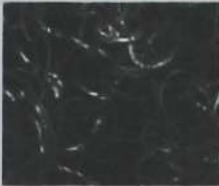

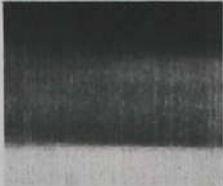









REFERENCE













1. Lahidji, B., *Determining Deflection for Metal Turning Operations*, Journal of Industrial Technology, Vol. 13, No. 2; 1997
2. Coker, S.A. & Shin, Y.C., *In-process Control of Surface Roughness Due to Tool Wear using a New Ultrasonic System*, International Journal Machine Tools Manufacturing, Vol. 36, No. , p. 411; 1996
3. S. Thamizhmanii, S. Hasan, *Analyses of roughness, forces and wear in turning gray cast iron*, Journal of achievement in Materials and Manufacturing Engineering, 17; 2006
4. Palanikumar, L. Karunamoorthy, R. Krathikeyan, *Assessment of factors influencing surface roughness on the machining of glass reinforced polymer composites*, Journal of Materials and Design, 27 862-871; 2006
5. Bruni, C., Forcellese, A, Gabrielli, F., and Simoncini, M., *Effect of the lubrication-cooling technique, insert technology and machine bed material on the workpart surface finish and tool wear in finish turning of AISI 420B*, International Journal of Machine Tools and Manufacture, 46, 12-13, October, 1547-1554; 2006
6. Pavel, R., Marinescu, I., Deis, M., and Pillar, J., *Effect of tool wear on surface finish for a case of continuous and interrupted hard turning*, Journal of Materials Processing Technology, 170, 1-2, December, 341-349; 2005
7. El-Axir, M.H. and Ibrahim, A.A., *Some surface characteristics due to center rest ball burnishing*, Journal of Materials Processing Technology, 167, 1, August 2005, 47-53; 2005
8. Thomas, M., and Beauchamp, Y., *Statistical investigation of modal parameters of cutting tools in dry turning*, International Journal of Machine Tools and Manufacture, Volume 43, 1093-1106; 2003













9. Kalpakjian, S., and Schmid, S., *Manufacturing Engineering And Technology*, 5th, PEARSON Prentice Hall; 2006
10. John cooper and Bruce DeRuntz, *The Relationship between the Workpiece Extension Length/Diameter Ratio and Surface Roughness in Turning Applications*, Journal of Industrial Technology, Volume 23, Number 2; 2007
11. Wang, Z., *Chatter Analysis of Machine Tool Systems in Turning Processes*, Ph.D. Thesis, National Library of Canada, Acquisitions and Bibliographic Services, 395 Wellington Street, Canada; 2001
12. Abburi, N.R. and Dixit, U.S., *A knowledge-based system for the prediction of surface roughness in turning process*, *Robotics and Computer-Integrated Manufacturing*, 363-372; 2006
13. Fidan, I., Kraft, R. P., Ruff, L. E. & Derby, S. J., *Designed experiments to investigate the solder joint quality output of a prototype automated surface mount replacement system*, *Components, Packaging, and Manufacturing Technology Part C: Manufacturing*, IEEE Transactions, V.21, No. 3, p. 172-181; 1998
14. Sandvick Coromant, *Metalcutting Technical guide*: Elanders 2005.
15. Alcoa Global Cold Finished Products, *Understanding Cold Finished Aluminum Alloys*, Massena (N.Y): 2007
16. Technical Data, *Surface Roughness*, Excerpt from JIS B 0601 and JIS B 0031: 1994.
17. Kalpakjian S. and Schmid Steven R., *Manufacturing Engineering and Technology*, Pearson Education Asia: 2000.
18. Douglas C. Montgomery, *Introduction to Statistical Quality Control*, 5th edition, John Wiley & Sons, Inc, page 555-600; 2005
19. Douglas C. Montgomery, *Introduction to Statistical Quality Control*, 5th edition, John Wiley & Sons, Inc, page 611-621; 2005
20. DMG Gildemeister, *CNC Universal Lathes CTX 10 Series*, DMG Vertriebes und Service GmbH: 2008
21. General Catalogue, *Performance Cutting Tools*, Sumitomo Electrical Hardmetal: 2007-2008.
22. Mitutoyo Catalogue, *Mitutoyo Surface Roughness Tester SJ-400*, Mitutoyo Corporation: 2006
23. D.D. Steppan, J. Werner, R.P. Yeater, *Essential regression and experimental design for chemists and engineers*, 1998.



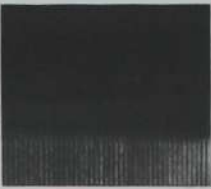






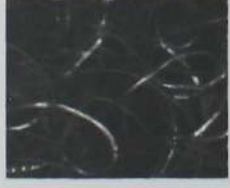


24. Safeen Y. Kassab* Younis K. Khoshnaw, *The Effect of Cutting Tool Vibration on Surface Roughness of Workpiece in Dry Turning Operation*, Eng. & Technology, Vol.25, No.7; 2007
25. Safeen Y. Kassab* Younis K. Khoshnaw, *The Effect of Cutting Tool Vibration on Surface Roughness of Workpiece in Dry Turning Operation*, Eng. & Technology, Vol.25, No.7; 2007
26. Beauchamp, Y., Thomas, M., and Masounave, J., *An experimental design for surface roughness and built-up edge formation in lathe dry turning*, International Journal of Quality Science 2 (3), 167–180; 1997
27. Kishawy, H.A., and Elbestawi, M.A., *International Journal of Machine Tools and Manufacture* 39, 1017–1030; 1997
28. Lambert, B. K., Determination of metal removal rate with surface finish restriction." *Carbide and Tool Journal*, 23, 16–19; 1983
29. Kwon, W.T., and Choi, D., *Radial immersion angle estimation using cutting force and pre-determined cutting force ration in face milling*, International Journal of Machine Tool and Manufacture, 42, 1649–1655; 2002
30. ISO 3685:1993, Tool-life testing with single-point turning tools, 1993.
31. E.M. Rubio, A.M. Camacho, J.M. Sanchez-Sola and M. Marcos, *Chip arrangement in the dry cutting of aluminum alloys*, Journal of achievement in materials and manufacturing engineering, volume 16, issues 1-2; 2006.













Appendix B: Data of Chip Formation, Tool Wear and Surface Roughness









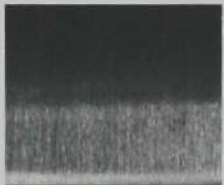



	CHIP FORM	TOOL WEAR	SURFACE ROUGHNESS
1			
A 180, B 0.07, C 0.1, D 22,			
	4.3 - Snarled	Crater Wear (100x)	Ra 0.43
2			
A 280, B 0.07, C 0.1, D 22,			
	4.3 - Snarled	Crater Wear	Ra 0.32
3			
A 180, B 0.17, C 0.1, D 22,			
	1.3 - Snarled	Crater Wear	Ra 1.18
4			
A 280, B 0.17, C 0.1, D 22,			
	2.3 - Snarled	Crater Wear	Ra 0.99












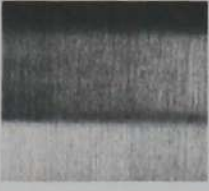
	CHIP FORM	TOOL WEAR	SURFACE ROUGHNESS
5			
A 180, B 0.07, C 0.2, D 22,			
	2.3 - Snarled	Crater Wear	Ra 0.52
6			
A 280, B 0.07, C 0.2, D 22,			
	2.3 - Snarled	Crater Wear	Ra 0.33
7			
A 180, B 0.17, C 0.2, D 22,			
	1.3 - Snarled	Crater Wear	Ra 1.26
8			
A 280, B 0.17, C 0.2, D 22,			
	1.3 - Snarled	Crater Wear	Ra 0.95

	CHIP FORM	TOOL WEAR	SURFACE ROUGHNESS
9			
A 180, B 0.07, C 0.1, D 52,			
	2.3 - Snarled	Crater Wear	Ra 1.12
10			
A 280, B 0.07, C 0.1, D 52,			
	2.3 - Snarled	Crater Wear	Ra 0.97
11			
A 180, B 0.17, C 0.1, D 52,			
	1.3 - Snarled	Crater Wear	Ra 1.38
12			
A 280, B 0.17, C 0.1, D 52,			
	1.3 - Snarled	Crater Wear	Ra 1.12

	CHIP FORM	TOOL WEAR	SURFACE ROUGHNESS
13			
A 180, B 0.07, C 0.2, D 52,			
	2.3 - Snarled	Crater Wear	Ra 1.17
14			
A 280, B 0.07, C 0.2, D 52,			
	1.3 - Snarled	Crater Wear	Ra 0.74
15			
A 180, B 0.17, C 0.2, D 52,			
	1.3 - Snarled	Crater Wear	Ra 1.60
16			
A 280, B 0.17, C 0.2, D 52,			
	2.3 - Snarled	Crater Wear	Ra 0.81

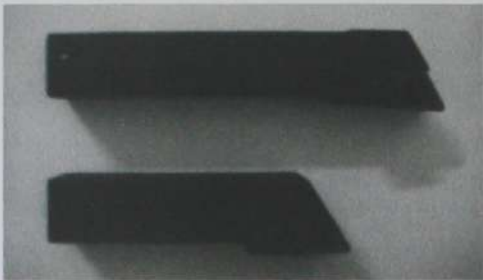
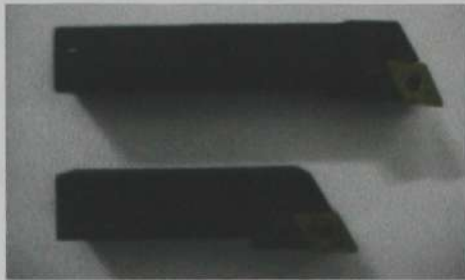


	CHIP FORM	TOOL WEAR	SURFACE ROUGHNESS
17			
A 230, B 0.11, C 0.15, D 37,			
	1.3 - Snarled	Crater Wear	Ra 0.73
18			
A 230, B 0.11, C 0.15, D 37,			
	2.3 - Snarled	Crater Wear	Ra 0.61
19			
A 230, B 0.11, C 0.15, D 37,			
	1.3 - Snarled	Crater Wear	Ra 0.70
20			
A 230, B 0.11, C 0.15, D 37,			
	1.3 - Snarled	Crater Wear	Ra 0.52

	CHIP FORM	TOOL WEAR	SURFACE ROUGHNESS
21			
A 230, B 0.12, C 0.1, D 37,			
	2.3 - Snarled	Crater Wear	Ra 0.57
22			
A 230, B 0.11, C 0.2, D 37,			
	2.3 - Snarled	Crater Wear	Ra 0.60
23			
A 230, B 0.12, C 0.15, D 22,			
	1.3 - Snarled	Crater Wear	Ra 0.62
24			
A 230, B 0.12, C 0.15, D 52,			
	1.3 - Snarled	Crater Wear	Ra 0.81




	CHIP FORM	TOOL WEAR	SURFACE ROUGHNESS
25			
A 230, B 0.12, C 0.15, D 37,			
	1.3 - Snarled	Crater Wear	Ra 0.62
26			
A 230, B 0.12, C 0.15, D 37,			
	1.3 - Snarled	Crater Wear	Ra 0.83
27			
A 230, B 0.12, C 0.15, D 37,			
	1.3 - Snarled	Crater Wear	Ra 0.65
28			
A 230, B 0.12, C 0.15, D 37,			
	1.3 - Snarled	Crater Wear	Ra 0.54

Appendix C: Tools & Inserts, Material, and Equipments use in Experiment

Tools and Inserts

	
<p>Cutting tools</p>	<p>Cutting tools & inserts</p>
	
<p>Inserts</p>	<p>Insert attached on cutting tool</p>

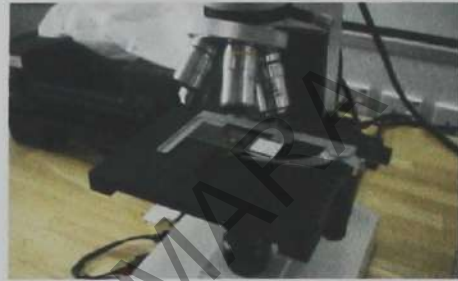
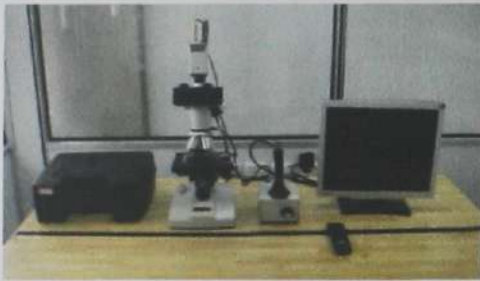
Materials

		
<p>Unmachined Bar</p>	<p>Machined Bar</p>	<p>Materials</p>

Equipments



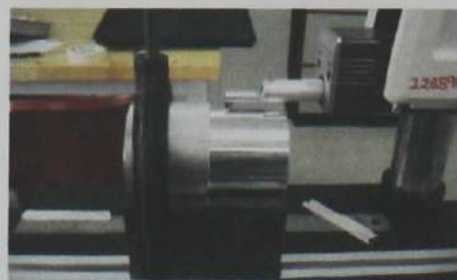
CNC Turning DMG Glidimiester



Video optical microscope (KKTM Balik Pulau)

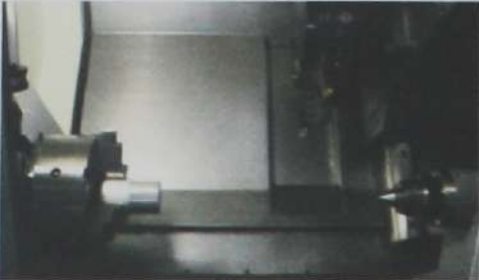


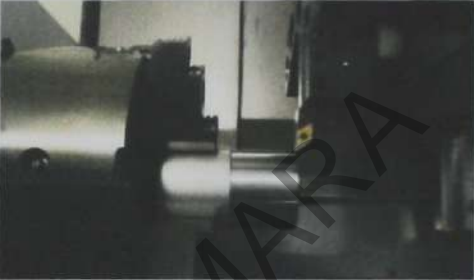
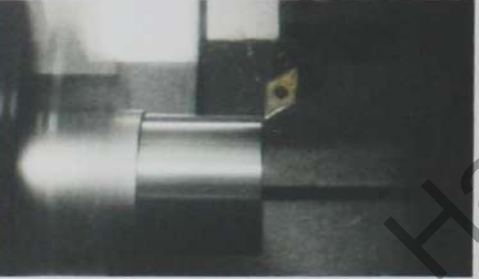
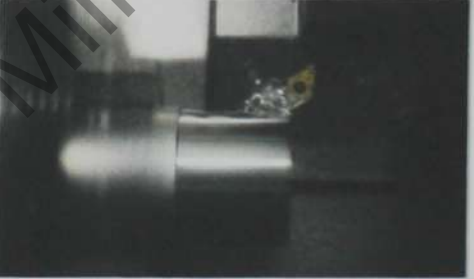




Video optical microscope (MSI Kulim)



Mitutoyo surface roughness tester

Others

	
Experiment set-up	Cutting tools attached on turret
	
Cutting tools 52 mm	Cutting tools 22 mm
	
Perform cutting	Perform cutting
	
Perform cutting	Perform cutting